Production routes to tailor the performance of cellulose nanocrystals

Oriana M. Vanderfleet[1,2] *and Emily D. Cranston*[2,3] ✉

Abstract | Cellulose nanocrystals (CNCs) are bio-based, high aspect ratio nanoparticles that are industrially produced in tonne-per-day quantities across the globe. CNCs can be used to improve the performance of a large range of materials such as emulsions and foams, biomedical devices, electronics and sensors, high-viscosity fluids and polymer composites. Their ability to do so, however, is highly dependent on the way they are produced. In this Review, we assess the properties of CNCs from more than 30 production routes and 40 biomass sources to help CNC users select the right material for their desired application. CNCs produced by various methods are evaluated against three target properties: colloidal stability, size and crystallinity index. Alternative production routes and/or starting materials are suggested to overcome challenges associated with CNC use, including increasing compatibility with hydrophobic materials, resistance to thermal degradation and colloidal stability in high ionic strength environments. Additionally, we discuss industrial production of CNCs, as well as considerations for increasing the yield and reducing the environmental impact of these processes. Overall, this Review guides researchers and CNC users towards a deeper understanding of how production processes can be modified to control CNC properties and subsequently tailor their performance.

Cellulose nanocrystals (CNCs) were first produced in 1947 by Nickerson and Habrle[1]. Cellulose was exposed to either sulfuric acid or hydrochloric acid at boiling temperatures, which was found to preferentially degrade less-ordered regions within the native cellulose structure. The remaining crystalline regions, referred to as 'cellulose micelles' and consisting of packed cellulose chains approximately 280 glucose units long, were further studied[2] and imaged[3] by Rånby et al. in 1949 and 1951, respectively. Following these studies, Mukherjee and Woods outlined the importance of acid concentration in CNC production and introduced the now commonly used 64 wt% sulfuric acid hydrolysis method[4]. Despite these early reports, there was a 40-year gap in research before scientific interest in CNCs was reignited in the 1990s; a timeline detailing research and development milestones is provided in FIG. 1. As CNC research progressed, many terms were used to identify these cellulosic nanomaterials, including 'hydrocellulose'; cellulose 'sols', 'monocrystals', 'micro(crystallites)', 'microcrystals', '(nano)whiskers', 'nanowires'; and 'nanocrystalline cellulose'. In 2017, standard terms and definitions were published, which concretized the term 'cellulose nanocrystals' (CNCs)[5]. Owing to their high specific Young's modulus[6], ease of dispersion in polar solvents[7], liquid crystal tendencies[8] and non-toxicity[9], CNCs have attracted great attention and have applications ranging from biomedical devices, water purification technologies, energy production and storage, and food and cosmetic modifiers to composite and construction materials. CNCs are now produced industrially in tonne-per-day quantities and as such are suitable for high-volume, commercial applications[10–12]. The performance of CNCs in composite materials, in both liquid and solid forms, is heavily dependent on the methods used to produce them as well as the cellulosic source material. This Review explores different CNC production routes and how they can be used to control the performance of this bio-based nanomaterial to expand its use in applications.

Most commonly, CNCs are produced by sulfuric acid hydrolysis, whereby cellulose chains undergo two reactions: hydrolysis of glycosidic bonds and esterification of surface hydroxy groups[13]. The hydrolysis of glycosidic bonds, which occurs rapidly within the less-ordered regions of cellulose, decreases the length of cellulose chains until mostly crystalline regions remain. Simultaneously, a fraction of the surface hydroxy groups are esterified to form sulfate half-ester groups that are anionic under practical working solution conditions. (CNCs produced from sulfuric acid hydrolysis are also called 'sulfated CNCs' as a result of this surface esterification and are sometimes erroneously referred to as 'sulfonated CNCs', which is incorrect, because it would require a

[1]*Department of Chemical Engineering, McMaster University, Hamilton, ON, Canada.*

[2]*Department of Wood Science, The University of British Columbia, Vancouver, BC, Canada.*

[3]*Department of Chemical and Biological Engineering, The University of British Columbia, Vancouver, BC, Canada.*

✉*e-mail: emily.cranston@ubc.ca*

https://doi.org/10.1038/s41578-020-00239-y

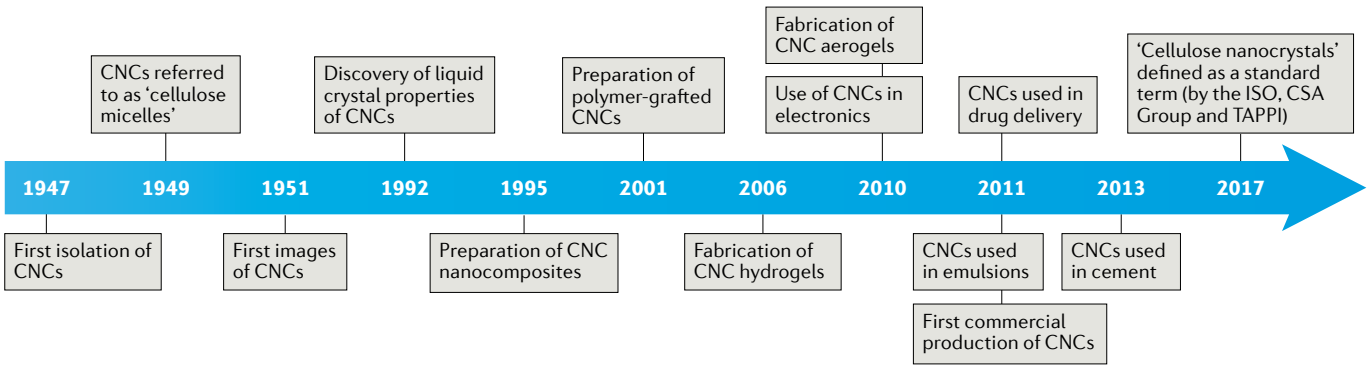

Fig. 1 | **Research milestones and terminology progression of CNCs.** A timeline detailing cellulose nanocrystal (CNC) production[1], imaging[3], liquid crystalline properties[8], nanocomposites[228], polymer grafting[64], hydrogels[233], aerogels[234], electronics[235], drug delivery[236], emulsions[237], cements[238] and industrial production as well as the standardization of CNC terminology[5].

carbon–sulfur bond, not a carbon–oxygen–sulfur bond, which has never been shown experimentally.) As a result of the two mechanisms occurring during acid hydrolysis, CNCs possess three crucial properties: colloidal stability in aqueous suspensions, nanoscale dimensions (with rod-like shape and high aspect ratio) and a high crystallinity index (FIG. 2). The first property stems from electrostatic repulsion between neighbouring CNCs, and the last two properties result from the degradation of disordered regions in cellulose during hydrolysis. For many CNC applications, these target properties are essential.

Despite the prevalent use and widespread industrial production of sulfated CNCs from cotton and wood pulp, many alternative production routes have emerged. Importantly, they are all chemical isolation methods based on acid hydrolysis or oxidation, in contrast to the mechanical methods (sometimes combined with enzymatic or chemical pretreatment) used to produce the longer, fibrillated, heterogeneous and less crystalline form of nanocellulose, namely cellulose nanofibrils (CNFs). Research efforts related to CNC production are often motivated by some of the challenges which limit the use of sulfated CNCs, such as their hydrophilic character[14], their tendency to aggregate in high ionic strength environments[15] and their lack of thermal stability[16]. Additionally, some efforts are focused on using low-value biomass sources[17–19], increasing the yield[20–22] or reducing the environmental impact[23,24] of CNC production routes. To accomplish these goals, a variety of mineral acids[25,26] and organic acids[24,27], as well as mixed acids[16,28,29], have been used to produce CNCs. Moreover, acid-free processes such as oxidation[30,31], enzymatic hydrolyses[32–34] and ionic liquid-mediated technologies[35–39] have been investigated. These new production routes, combined with the study of dozens of starting cellulose sources[40], have resulted in CNCs with differing surface chemistry, surface charge density and morphology. Here, we examine the ability of alternative production routes and cellulose sources to achieve the desired CNC target properties. Furthermore, production routes capable of tailoring additional properties are discussed as we aim to support the broadening of application areas for CNCs and guide CNC end users to select appropriate methods and materials.

Production routes and biomass sources

Target properties. The performance of CNCs can be roughly evaluated on the basis of the three target properties: aqueous colloidal stability, size and crystallinity index (FIG. 2). If particles are well dispersed and resist aggregation and sedimentation in a liquid medium, they are deemed colloidally stable. For CNCs, this stability is governed by Derjaguin–Landau–Verwey–Overbeek (DLVO) theory (the balance of van der Waals attraction and electrostatic repulsion) or sometimes results from steric or electrosteric repulsion; for example, with hairy nanocelluloses[41]. High colloidal stability is essential to produce uniform dispersions with predictable and consistent performance. For example, material processing, viscosity and shelf life are highly dependent on colloidal stability. Charged CNC colloidal stability can be inferred by measuring electrophoretic mobility and subsequently calculating the zeta potential following Smoluchowski's theory or the recently reported, and more accurate, modified Oshima–Overbeek equation[42]. Absolute zeta potential values up to 10 mV are categorized as highly unstable, greater than 10 and up to 20 mV as relatively stable, greater than 20 and up to 30 mV as moderately stable, and magnitudes exceeding 30 mV are considered highly stable[43]. Colloidal stability can also be assessed using light transmission through a CNC suspension, or by measuring apparent particle size by dynamic light scattering (DLS), over time, to determine whether and when aggregation or sedimentation occurs[44].

The dimensions and shapes of CNCs are also key properties that govern their performance: CNCs with nanoscale lengths and high aspect ratios are desirable. Nanoscale dimensions provide CNCs with high surface-area-to-volume ratios, which means that adding a small amount to a material greatly affects its properties, and for a given mass, the smaller the nanoparticles, the greater the number of available sites for chemical reactions, and adsorption or release of other chemical moieties. Furthermore, high aspect ratios allow CNCs to self-assemble into liquid crystalline phases, adopt robust mesh structures to stabilize interfaces and form percolated networks; for example, in polymer nanocomposites[8,45]. CNC size is measured by microscopy techniques, primarily atomic force microscopy (AFM)

and transmission electron microscopy (TEM), calculated from small-angle neutron or X-ray scattering[15,46] or inferred from light scattering; for example, DLS or laser light scattering[44,47,48]. While DLS is a straightforward measurement, the results are often reported as hydrodynamic radii, meaning the Stokes–Einstein equation relates the translational diffusion coefficient to particle size under the assumption of hard, spherical particles[43]. Although modified Stokes–Einstein equations are available for cylindrical particles[43] (and these report two dimensions: length and diameter), they are seldom used in the analysis of CNC size. Furthermore, DLS measurements are heavily weighted by aggregates[43]. Microscopy is more accurate but time-consuming and is not immune to inaccuracies (such as tip broadening effects in AFM or staining issues in TEM)[49]. Typically, CNCs have microscopy lengths of 100–200 nm and cross sections of 5–20 nm, or apparent sizes of less than 100 nm by DLS[10].

The third property used to assess the performance of CNCs is their crystallinity index, which indicates the degree of order of the cellulose chains that make up the particles themselves and indicates the completeness of the reaction used in their production. Crystallinity of CNCs is primarily linked to mechanical properties but can also affect chemical reactivity and thermal stability. While CNCs are generally in the native cellulose I allomorph, variations in the starting material or process can accidentally or purposely introduce cellulose II[10,50,51]. The crystallinity index of CNCs can be determined through a variety of techniques, including Raman spectroscopy, NMR spectroscopy and X-ray diffraction (XRD)[52,53], although there is some controversy over which technique is most accurate. Recently, a review outlined each characterization technique and its applicability in discovering cellulosic crystal structures[44]. For the purpose of this Review, only XRD measurements are considered because XRD is the most widely used technique and does not require calibration. Despite its widespread use, all crystallinity index values determined by XRD are not equal as a consequence of differences in sample preparation and curve fitting procedures. Several methods exist to translate X-ray diffractograms into a single crystallinity index (also called the 'degree of crystallinity' and given as a percentage). For the purposes of this Review, we define highly crystalline as a crystallinity index greater than 80%. Nevertheless, because sample preparation and instrumentation make it difficult to compare reported values[54], the comparisons in the following sections are only approximate.

Production routes. The most well-studied and most widely used protocol to produce CNCs uses concentrated sulfuric acid to hydrolyse and esterify cellulose[55] (FIG. 3a) in less than 2 h with yields in the 20–75% range. Sulfuric acid is a strong acid, and the high concentration of protons attacks the glycosidic bonds faster in less ordered regions of cellulose. As these bonds are broken, the cellulose chains become shorter and the average degree of polymerization decreases until the disordered regions have been fully degraded and the levelling off degree of polymerization (LODP) is reached[1,56] (FIG. 3b). If the hydrolysis reaction is allowed to continue, the degree of polymerization of the cellulose chains, and the CNC length, will continue to decrease but very slowly compared with the initial decrease. Generally, when the LODP is reached, the acid and cellulose slurry is quenched to terminate the reaction. At this stage, the sulfated CNCs can be easily centrifuged into a pellet because the high ionic strength of the quenched slurry screens electrostatic repulsion, and the acid is subsequently removed by centrifugation and dialysis. Lastly, the aqueous CNC suspension is sonicated with an ultrasonic probe (to unhinge the crystals) and filtered (to remove any unhydrolysed cellulose or impurities). The common laboratory-scale process to produce CNCs (FIG. 3c) has similarities to industrial-scale production, such as acid concentration, time, temperature and mixing; however, the quenching, purification, neutralization and drying steps have required optimization for larger-scale production. The resulting CNCs are highly crystalline nanoparticles with deprotonated sulfate

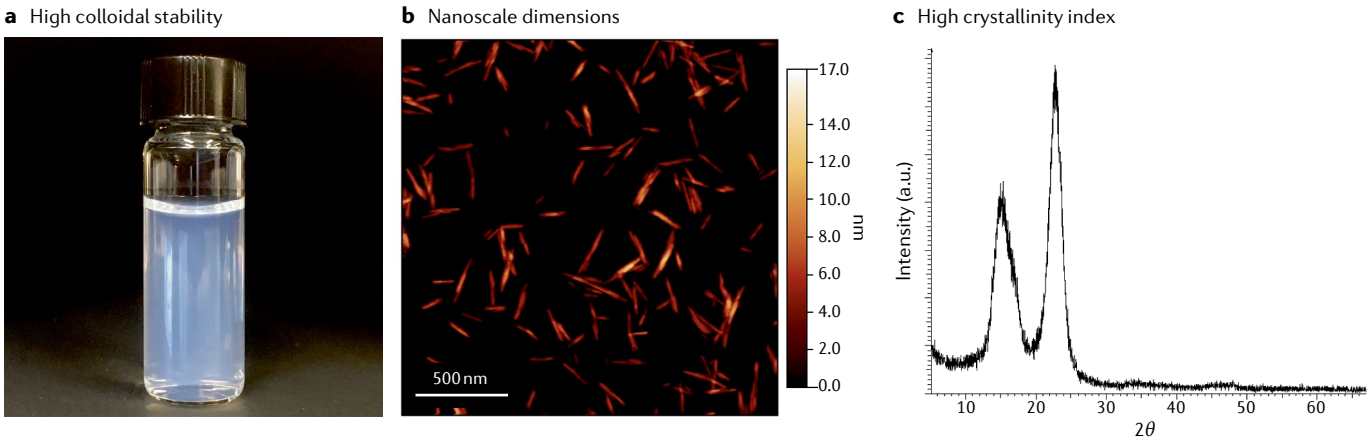

Fig. 2 | **CNC target properties. a** | A colloidally stable 1 wt% aqueous cellulose nanocrystal (CNC) dispersion[44]. **b** | An atomic force microscopy image showing the whisker-like shape of CNCs[127]. **c** | An X-ray diffraction pattern of highly crystalline CNCs in the native cellulose I crystal structure[44]. Panels **a**,**c** reprinted with permission from REF.[44], Royal Society of Chemistry. Panel **b** reprinted with permission from REF.[127], American Chemical Society.

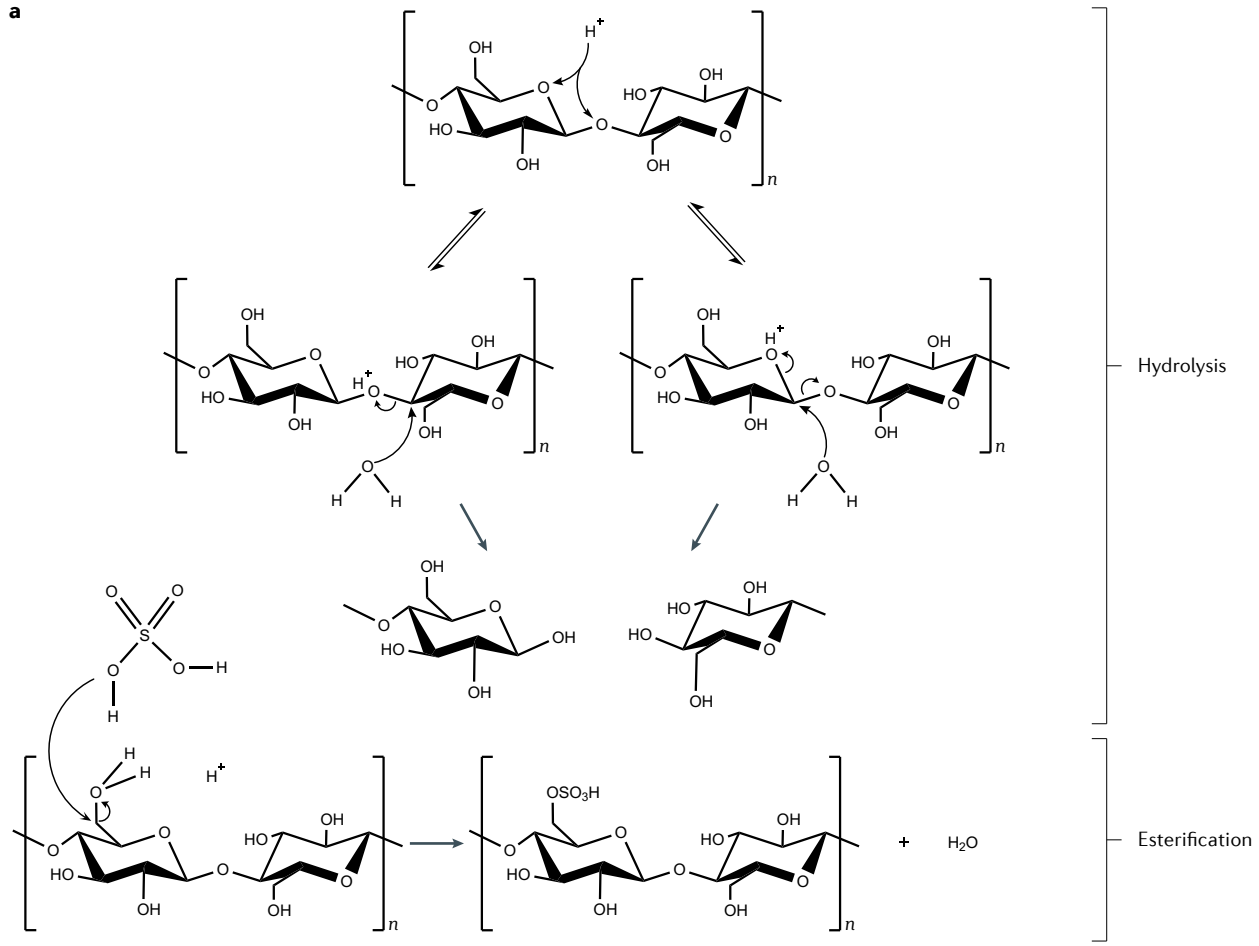

Fig. 3 | **Physical and chemical mechanisms of cellulose hydrolysis to produce CNCs. a** | Mechanism for hydrolysis and esterification of cellulose subjected to concentrated sulfuric acid. **b** | The levelling off degree of polymerization of cellulose chains during sulfuric acid hydrolysis. **c** | The laboratory-scale production of cellulose nanocrystals (CNCs).

half-ester surface groups which meet all three target properties discussed in the previous section.

Despite the uniformity, reproducibility, high yield, stability and predictable properties of CNCs made with sulfuric acid, many researchers have investigated alternative production routes. The viability of these methods can be assessed by evaluating the target properties of the resulting CNCs (TABLE 1). Additionally, the yield is assessed because a high yield is a requirement for any economically feasible industrial process. Besides sulfuric acid, several other mineral acids have been used to produce CNCs. Hydrochloric acid, hydrobromic acid and

Table 1 | **CNC production routes and resulting properties**

Production route	Reagents	CNC surface chemistry	Colloidal stability	Size (CNC length)	Crystallinity index (%)	Yield (%)	Refs[a]
Mineral acids	Sulfuric acid		Highly stable	Nano	70–93	20–75	1,10,72,80
	Sulfuric acid and ultrasonication		NR	Nano; some aggregates	77–81	53–71	125
	Phosphoric acid		Unstable	Nano	81–97	76–80	25,57
	Hydrochloric acid (liquid)	Unmodified	Uncharged	Nano; very aggregated	86–88	80–93	1,22,195
	Hydrochloric acid (vapour)	Unmodified	Uncharged	Nano; very aggregated	58–64	97	20
	Hydrochloric acid hydrolysis of TEMPO-oxidized CNFs		NR	Nano	78–80	69–85	65
	Hydrobromic acid	Unmodified	Uncharged	Nano; very aggregated	91	70	26
	Phosphotungstic acid	Unmodified	Unstable	Nano and micro	80–85	20–88	21,196
Organic acids	Oxalic acid		Highly stable	Nano and micro	80–83	1–25	24
	Oxalic acid dihydrate and mechanical disintegration		NR	Nano; some aggregates	74–79	84–99	27,58
	Maleic acid		Highly stable	Nano; some aggregates	72–81	1–13	24,59
	Formic acid		Unstable	Nano and micro; very aggregated	66–75	70–78	60
Acid blends	Phosphoric and sulfuric acids	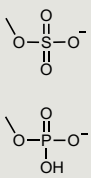	Relatively stable	Nano	94–95	NR	16
	Sulfuric and hydrochloric acids		Highly stable	Nano; some aggregates	83	NR	197
	Hydrochloric and citric acids		NR	Nano; some aggregates	78	5–20	151
	Hydrochloric and malonic acids		NR	Nano; some aggregates	75	5–20	151
	Hydrochloric and malic acids		NR	Nano; some aggregates	78	3–20	151
	Hydrochloric and acetic acids	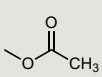	NR	Nano; very aggregatedd	NR	15–35	164
	Hydrochloric and butyric acids	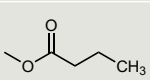	NR	Nano; very aggregated	NR	22	164

Table 1 (cont.) | **CNC production routes and resulting properties**

Production route	Reagents	CNC surface chemistry	Colloidal stability	Size (CNC length)	Crystallinity index (%)	Yield (%)	Refs[a]
Acid blends (cont.)	Hydrochloric and 2-bromopropionic acids	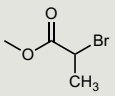	NR	Nano; some aggregates	78	46	28
	Hydrochloric and 3-mercaptopropionic acids	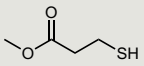	NR	Nano	81	50	28
	Hydrochloric and 4-pentenoic acids	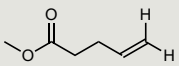	NR	Nano	65	48	28
	Hydrochloric and 2-propynoic acids	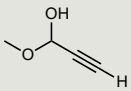	NR	Nano	74	62	28
	Hydrochloric and nitric acids		Highly stable	Nano; some aggregates	73–82	90–91	198
Oxidizing agents	TEMPO-mediated oxidation and ultrasonication		Highly stable	Nano	60–80	69–94	30
	Sodium periodate		Sterically stabilized	Nano	NR	50	41
	Sodium periodate and sodium borohydride		Sterically stabilized	Nano	NR	60–79	66
	Ammonium persulfate		NR	Nano	64–91	14–81	31
	Hydrogen peroxide		Highly stable	Nano; some aggregates	NR	20–50	103
Ionic liquids	1-Butyl-3-methylimidazolium hydrogen sulfate		NR	Nano and micro; very aggregated	82–96	NR	36,70
	1-Ethyl-3-methylimidazolium acetate	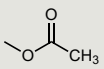	Uncharged	Nano; very aggregated	73	44	35
	Tetrabutylammonium acetate	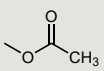	Uncharged	Nano and micro; very aggregated	51	NR	37
	Choline chloride and oxalic acid dihydrate, followed by mechanical disintegration (deep eutectic solvents)		NR	Nano; very aggregated	66–71	68–78	38
	Choline chloride, oxalic acid dihydrate and *p*-toluenesulfonic acid (deep eutectic solvents)		NR	Nano; very aggregated	57	66	39
Other	Subcritical water	Unmodified	Uncharged	Nano	79	22	23
	Sulfur dioxide and ethanol (AVAP®)	Unmodified	Uncharged	Nano; very aggregated	93	24	67

CNC, cellulose nanocrystal; CNF, cellulose nanofibril; NR, not reported; TEMPO, (2,2,6,6-tetramethylpiperidin-1-yl)oxyl. [a]References cited indicate pioneering work with a given production route or a study focused on process optimization.

phosphotungstic acid hydrolyses produce high yields of CNCs with high degrees of crystallinity[20–22,26]. The resulting CNCs, however, are uncharged and form large aggregates; this is undesirable for most applications as they lose the advantages of being nano-sized and cannot form uniform dispersions with consistent properties. If yield is of primary concern, gaseous HCl hydrolysis gives a 97% yield from cotton, which is attributed to swelling

and crystallization of the disordered cellulose regions during the relatively slow process, which is a significant improvement over the yields of industrially produced CNCs[20]. The challenge is that the CNCs produced from HCl vapour hydrolysis need postmodification (with (2,2,6,6-tetramethylpiperidin-1-yl)oxyl, commonly known as TEMPO-mediated oxidation, for example) to impart surface charge, colloidal stability and individualized nanoparticles. While CNCs produced with phosphoric acid, a weak acid, do possess phosphate half-ester groups[25], the increase in colloidal stability over uncharged CNCs from other mineral acid hydrolyses is small[25,57]. Although there is little functional difference, CNCs can be classified as either uncharged or unstable (TABLE 1), the latter of which have some surface charge groups but not enough to impart the targeted colloidal stability. Therefore, if a single mineral acid is to be used, CNCs with high colloidal stability, uniform nanoscale lengths and high crystallinities can be produced only with sulfuric acid.

Lately, interest has grown in using organic acids to produce CNCs with new surface functionalities. While CNCs can be made with these processes, the degree of crystallinity which can be achieved is generally lower than that of CNCs made with mineral acids[24,27,58–60]. Furthermore, some organic acid hydrolyses sacrifice yield or colloidal stability. While CNCs made with oxalic acid or maleic acid are colloidally stable, their yields are low[24]. Conversely, CNCs produced with formic acid have higher yields, yet the resulting CNCs have low colloidal stability and form aggregates[60].

To overcome some of the drawbacks of organic acids, weak acids or mineral acids that do not impart surface charge, mixtures of acids have been used to produce CNCs. Most acid blends combine a strong mineral acid (hydrochloric acid or sulfuric acid) with an organic acid or a weak mineral acid because the kinetics of cellulose hydrolysis are largely governed by acid concentration, which is directly related to proton concentration[55]. When strong acids are used to produce CNCs, higher proton concentrations result in a rapid and uniform hydrolysis. If weak acids are used alone, equilibrium dictates that the acid groups are not fully dissociated, and sufficiently high proton concentrations cannot be achieved. Therefore, by combining multiple acids, highly crystalline nanoscale particles can be achieved owing to the strong acid contribution, while surface chemistry can be tailored by the choice of the weaker acid. In some cases, two esterifying acids have been used. For example, blends of sulfuric acid and phosphoric acid produce CNCs with both sulfate and phosphate groups[16]. In most cases, however, hydrochloric acid is used in conjunction with organic acids, and these production routes generally produce nanoscale CNCs with moderately high crystallinities. The colloidal stability of these acid blend-produced CNCs has not been thoroughly characterized; however, some samples, particularly those made with 3-mercaptopropionic acid, 4-pentenoic acid and 2-propynoic acid, appear well dispersed when imaged by AFM[28]. Overall, the use of acid blends to produce CNCs which meet all target properties and have a variety of surface chemistries is a growing research area which promises to expand the use of CNCs in diverse applications.

Importantly, CNCs can be produced without acid; common methods to do so include oxidation reactions, enzymatic hydrolyses or production with ionic liquids or subcritical water. Of these methods, oxidation reactions yield some of the best results: CNCs are consistently colloidally stable, have nanoscale dimensions and have high crystallinities[30,31,41]. Furthermore, extremely high densities of surface carboxyl groups can be achieved, particularly in the case of TEMPO-oxidized CNCs and CNCs made with ammonium persulfate[30,61]. In this Review, we attempt to distinguish surface modification methods from production routes and note the difference between TEMPO-oxidized CNCs obtained as a post-production surface modification on acid-hydrolysed CNCs[62–64] (not discussed herein) and those produced primarily with TEMPO. For example, the latter can be achieved through extensive sonomechanical treatment of TEMPO-oxidized pulp or microcrystalline cellulose[30], or through an acid hydrolysis of TEMPO-oxidized CNFs[65] (TABLE 1). Alternatively, sterically stabilized CNCs can be produced with use of sodium periodate as the oxidizing agent; these CNCs have peeled or fibrillated cellulose surface chains with aldehyde (or converted hydroxy, carboxyl or amine) groups[41,66]. Transition metal-catalysed oxidative routes and sulfur dioxide with ethanol (American value-added pulping (AVAP®) process)[67] have also been used to produce nanocellulose mixtures with a significant fraction of CNCs[10,68]. CNCs with carboxyl groups and CNCs with aldehyde groups present opportunities for surface modification that cannot be achieved with sulfate groups, such as carbodiimide coupling and chemical crosslinking via hydrazone chemistry[69].

Beyond oxidative methods, no other acid-free methods to produce CNCs have been successful at achieving all three target properties. CNCs produced with ionic liquids are generally uncharged or colloidally unstable and therefore form large aggregates[35–37,70]. Furthermore, they often have lower crystallinities than CNCs made with sulfuric acid[35,37]. CNCs have more recently been produced with deep eutectic solvents, which are a subcategory of ionic liquids[38,39] (for example, choline chloride combined with oxalic acid dihydrate), and although these solvents impart carboxyl groups onto the CNC surfaces, some aggregates are still present and the crystallinity indices are low (TABLE 1). Similarly, CNCs produced with subcritical water are uncharged, despite having high crystallinities[23]. Lastly, at this stage of research and development, CNCs produced with enzymatic hydrolyses do not meet any of the three target properties: they are colloidally unstable, nanoscale dimensions are not consistently achieved and they have low crystallinities[32–34]. However, we believe that some of these methods offer promise, particularly from a green chemistry and cost perspective and we expect future research to be focused in this area. These results outline the difficulty in producing high-performing CNCs via alternative production routes. It is unsurprising that sulfuric acid hydrolysis and oxidative methods are the most common processes reported in the literature and are the major focus of scale-up efforts.

Optimization of production routes. Many efforts have been made to optimize the production of CNCs, particularly from sulfuric acid. Although some optimization studies focus on varying one reaction parameter at a time, many have used response surface methodology, which generates mathematical models capable of determining optimal reaction conditions[21,57,71–73]. The effects of hydrolysis parameters such as reaction time (10 min to 18 h), temperature (26–80 °C), acid concentration (16–68 wt%) and acid to pulp ratio (0.5–1.5 g pulp per millilitre of acid) on CNC surface charge density, size, crystallinity and yield have been evaluated[72–80]. Although maximizing CNC yield is often the focus of optimization studies, CNC performance is equally as important; ideal CNCs will have high colloidal stability in water (from high surface charge), nanoscale dimensions and high crystallinity while being produced from a high-yield process. In general, harsher hydrolyses (longer, hotter or more concentrated acid) produce CNCs with smaller sizes and more surface charge groups. The yield and crystallinity, however, have a parabolic relationship with hydrolysis harshness. If the hydrolysis is not harsh enough, disordered regions will remain unhydrolysed and only a few CNCs will be produced, while the rest of the initial cellulose mass is recovered as solid residue. If the hydrolysis is too harsh, however, crystalline regions begin to degrade, thus reducing both the yield and the degree of crystallinity[72,76–78,80].

Overall, the acid concentration is the dominant factor in determining CNC properties; the range of acid concentrations which can successfully produce CNCs is narrow, and the frequently used concentration of 64 wt% sulfuric acid is generally regarded as the optimal value[4,10,80] (higher concentrations risk significant swelling and dissolution of cellulose). The length of time and the temperature of the hydrolysis are also important factors; however, these can depend on the geometric set-up and scale of the reaction. Similar optimization studies have also been performed on other production routes, including hydrolyses with subcritical water[81], phosphoric acid[25,57] and maleic acid[71].

Sources of biomass. CNCs are most commonly produced from lignocellulosic sources such as wood pulp, grasses and cotton. In some regions, however, wood is scarce, while other cellulose sources are more plentiful. As a result, CNCs have been successfully produced from agricultural waste products such as sugar cane bagasse, apple pomace, garlic straw, pineapple leaf and tomato peel, to name a few[19,82–85] (TABLE 2). For each new biomass source, a process must be developed to isolate the cellulose from other components such as hemicelluloses, lignin, inorganic compounds and waxes. For wood pulp, cotton and most plants, the cellulosic fraction is quite high; however, for agricultural residue, the cellulose yield after purification is typically only 30–40% and can be as low as 13%[18,85,86].

In general, CNCs from wood pulp and cotton sources are similar: they have lengths between 100 and 200 nm, which is due to the LODP of the fibres themselves (cotton fibres and bleached sulfite pulps have LODP values of 200–250 and 200–280, respectively)[56]. Despite their similarities, subtle differences in sizes (which are statistically insignificant) have been suggested: wood pulp CNCs appear slightly shorter[87]. This observation could explain why other properties, such as liquid crystalline self-assembly, viscosity, diffusion coefficients and surface activity, differ significantly[87]. Comparison of CNCs from softwood (spruce) and hardwood (eucalyptus) pulps, however, has indicated that the target properties are extremely similar if the CNCs are produced following the same protocol[75]. Some plants, such as ramie and hemp, have more crystalline cellulose fibres to begin with and higher LODP values (approximately 300–350)[56,88]. Theoretically, they should produce longer CNCs; however, inconsistent hydrolysis protocols between research groups make direct comparisons difficult. Noteworthy yields above 70% come from *Miscanthus* × *giganteus*[89], eucalyptus[80] and jute[90]. Although subtle differences exist among lignocellulosic starting materials, the effects of the hydrolysis conditions often prevail[91].

CNC production, however, is not limited to lignocellulosic biomass. CNCs have also been produced from tunicates (where the cellulose is found in the mantle or tunic of these sea animals) and algae[34] (TABLE 2). Additionally, bacterial cellulose can be produced from live cultures of Gram-negative acetic acid bacteria (for example, *Komagataeibacter xylinus*, formerly known as *Gluconacetobacter xylinus* and *Acetobacter xylinum*) or purchased as nata de coco, which is an edible coconut gel[34]. These starting materials tend to produce longer CNCs, which can have lengths exceeding 1 µm (REF.[75]). While CNCs from tunicates consistently have lengths in the micrometre range, CNCs from algae[92–95] and bacterial cellulose[96,97] can be closer in size to lignocellulosic CNCs, depending on the method used to produce them (TABLE 2). Although many uses would benefit from longer CNCs, use of tunicate cellulose as a starting material is infeasible for most large-scale applications owing to cost and the extensive precleaning and separation procedures needed; therefore, other routes to greatly increase the CNC aspect ratio would be welcomed. Overall, although some cellulose sources (particularly tunicates) produce CNCs with significantly different properties, many starting materials offer only subtle differences, which are even more difficult to compare when production routes differ as well.

Industrial production. Currently, CNCs are produced industrially by ten organizations[11,12,98] (TABLE 3), which have pilot, demonstration or semi-industrial plant facilities with production capacities in the kilogram-per-day to tonne-per-day range (on a dry weight basis). CelluForce Inc. is the world's largest producer of CNCs (since 2011), with Alberta-Pacific Forest Industries Inc., GranBio and Anomera Inc. following close behind and with the commissioning of new plants in progress. The first European CNC plant will be built by MoRe Research, a joint effort between Melodea Ltd, Holmen AB, and RISE Research Institute of Sweden AB, in Örnsköldsvik, Sweden (further production capacity and timeline information is currently unavailable). Smaller pilot-scale facilities are primarily operated by research organizations focused on process optimization (for consistency, purity, quality and economics)[99], novel

Table 2 | **Biomass sources used to produce CNCs and the nanoparticle size, crystallinity and yield**

Category	Source	Production route	Average size (CNC length)	Crystallinity index (%)	Extraction yield (%)	Refs[a]
Wood	Bleached eucalyptus kraft pulp	Sulfuric acid hydrolysis	100–250 nm	68–79	28–76	80
	Bleached softwood kraft pulp	Sulfuric acid hydrolysis	~150 nm	79–89	21–33	75,76
	Kimwipes	Sulfuric acid hydrolysis	~200 nm	87	NR	199
	Microcrystalline cellulose	Sulfuric acid hydrolysis	200–400 nm	NR	30	73
	Microfibrillated cellulose	Sodium periodate oxidation and sodium borohydride reduction	~60 nm	NR	60–79	66
	Mulberry branch bark	Sulfuric acid hydrolysis	400–500 nm	73	NR	200
	Sawdust waste	Sulfuric acid hydrolysis	~250 nm	90	15	201
	Spruce bark	Sulfuric acid hydrolysis	~200 nm	84	32	202
	TEMPO-oxidized cellulose nanofibres	Hydrochloric acid hydrolysis	~300 nm	78–80	69–85	65
Cotton	Cotton linter	Sulfuric acid hydrolysis	150–200 nm	90	NR	203
	Mercerized cotton (cellulose II)	Sulfuric acid hydrolysis and homogenization	~75 nm	62	30–35	51
	Waste cotton cloth	Sulfuric and hydrochloric acid hydrolysis	28–470 nm	47	56	204
	Whatman ashless filter aid	Sulfuric acid hydrolysis	~150 nm	93	NR	10
	Whatman no. 1 filter paper	Sulfuric acid hydrolysis	NR	NR	NR	205
Plants and grasses	Bamboo	Sulfuric acid hydrolysis	~100 nm	87	30	91
	Elephant grass	Sulfuric acid hydrolysis	150–300 nm	72–77	12–16	206
	Flax	Sulfuric acid hydrolysis	~300 nm	NR	NR	207
	Hemp	Sulfuric acid hydrolysis	100–200 nm	87–89	19	208,209
	Jute	TEMPO-mediated oxidation followed by mechanical treatment	100–200 nm	70	80	90
	Kenaf	Sulfuric acid hydrolysis	~150 nm	75–82	23–59	77
	Mengkuang leaves	Sulfuric acid hydrolysis	~200 nm	NR	28	210
	Miscanthus × *giganteus*	Sulfuric acid hydrolysis	~300 nm	78	75	89
	Ramie	Sulfuric acid hydrolysis followed by mechanical treatment	150–250 nm	NR	NR	211
	Sisal	Sulfuric acid hydrolysis	~250 nm	NR	30	129
	Southern cattail	Sulfuric acid hydrolysis	600–700 nm	74–80	NR	212
	Sunflower stalk	Sulfuric acid hydrolysis	150–200 nm	70	21	213
Agricultural waste	Apple pomace	Sulfuric acid hydrolysis followed by mechanical treatment	~30 nm	78	NR	19
	Banana pseudostems	Sulfuric acid hydrolysis	~400 nm	74	10	214
	Coconut husk	Sulfuric acid hydrolysis	~200 nm	62–66	NR	215
	Coffee husk	Sulfuric acid hydrolysis	~300 nm	92	NR	216
	Corncob	Sulfuric acid hydrolysis	200–300 nm	78–84	46–57	217
	Garlic straw	Sulfuric acid hydrolysis	~500 nm	69	20	218
	Mango seed	Sulfuric acid hydrolysis	~100 nm	91	23	219
	Onion skin	Sulfuric acid hydrolysis	150–350 nm	26–30	39–49	220
	Passion fruit peel	Sulfuric acid hydrolysis	~150 nm	78	58	221
	Pea hulls	Sulfuric acid hydrolysis	250–400 nm	NR	NR	222
	Peanut shell	Sulfuric acid hydrolysis	~100 nm	74	12	18
	Pineapple leaf	Sulfuric acid hydrolysis	~250 nm	73	65	84
	Pineapple peel	Sulfuric acid hydrolysis	~200 nm	61	21	223
	Pistachio shell	Sulfuric acid hydrolysis	~200 nm	66	50	224
	Potato peel	Sulfuric acid hydrolysis	~400 nm	85	41–42	225
	Rice husk	Sulfuric acid hydrolysis	150–300 nm	59	NR	86
	Rice straw	Sulfuric acid hydrolysis	100–300 nm	86–91	5–6	226
	Soy hulls	Sulfuric acid hydrolysis	100–150 nm	75	20	227
	Sugar cane bagasse	Sulfuric acid hydrolysis	~250 nm	88	58	17
	Tomato peel	Sulfuric acid hydrolysis	100–200 nm	81	16	85

Table 2 (cont.) | **Biomass sources used to produce CNCs and the nanoparticle size, crystallinity and yield**

Category	Source	Production route	Average size (CNC length)	Crystallinity index (%)	Extraction yield (%)	Refs[a]
Animals	Tunicate	Sulfuric acid hydrolysis	~1 µm	80	NR	34,228
Algae	*Cladophora*	Sulfuric acid hydrolysis	~4 µm	NR	NR	92
	Gelidium sesquipedale	Sulfuric acid hydrolysis	~300 nm	81–87	11–14	93
	Microdictyon tenuius	Hydrochloric acid hydrolysis	~1–10 µm	NR	NR	94
	Valonia macrophysa	Dry methanol and acetyl chloride (to produce hydrochloric acid in situ)	200 nm to several micrometres	NR	NR	95
Bacterial cellulose	*Komagataeibacter xylinus*	Sulfuric acid hydrolysis	~1 µm	72	NR	34,144

CNC, cellulose nanocrystal; NR, not reported; TEMPO, (2,2,6,6-tetramethylpiperidin-1-yl)oxyl. [a]References refer to the first publication using a given source material to produce CNCs that possess the target properties defined in this Review. In some cases, reviews or research articles focused on production routes or optimization are included.

production routes and the development of new purification techniques, drying methods and industrially feasible surface modification strategies. For example, process intensification was done by FPInnovations (the first organization to work on scale-up, in collaboration with McGill University's Pulp and Paper Research Centre in the early 2000s, which then joined forces with Domtar Inc. to create CelluForce Inc.) and the Forest Products Laboratory of the US Department of Agriculture. Although these organizations have provided CNCs for research and development, they do not sell products in large volumes. Formerly, the CNCs produced by the US Department of Agriculture's Forest Products Laboratory could be procured from the University of Maine's Process Development Center[100], but this is no longer the case: CNCs purchased from the University of Maine are now produced by CelluForce Inc.

Sulfuric acid hydrolysis remains the most common production route at the industrial scale — this process provides high-quality sulfated CNCs that meet the property targets discussed earlier and are the primary CNC type that have been used in commercial application development[10]. The innovations that were needed to move to this tonne-per-day production capacity included handling and recycling strong acids at scale, new membrane filtration systems for purification, and spray-drying of CNCs into a redispersible powder[101] for easier shipping and an extended shelf life. Recently, the first continuous sulfuric acid hydrolysis process was reported (replacing the batch process and using three times less acid) by InnoTech Alberta in conjunction with Alberta-Pacific Forest Industries Inc. (with engineering conducted by NORAM Engineering and Constructors Ltd)[102]. This continuous reactor process may offer significant savings in time, chemicals and energy costs.

The production of CNCs following oxidative routes is emerging as a highly scalable and cost-efficient process to make carboxylated CNCs (by Anomera Inc. and Blue Goose Biorefineries Inc.). These routes use dilute hydrogen peroxide[103] and transition metal-catalysed oxidation[104], respectively, and bear no resemblance to the ammonium persulfate oxidation method[31] patented by the National Research Council of Canada in 2011 and licenced by BioVision Inc. (turned Advanced Cellulosic Materials Inc. and now no longer operating). Another promising route to produce low-cost CNFs and CNCs is the GranBio AVAP® process, which uses (recyclable) ethanol and SO_2 to remove hemicelluloses, lignin, resins and extractives, while producing strong lignosulfonic acids, which then hydrolyse disordered cellulose to isolate a high-crystallinity end product[67]. The resulting CNCs (with unmodified cellulose surface chemistry) are combined with other products from the reaction (but can be size-fractionated) and either are bleached or may have deposited lignin to decrease the nanoparticle surface hydrophilicity. Low operating and capital costs, combined with standard unit operations and readily available chemicals, are a significant advantage.

Most commercial production routes claim (to various extents) that they are feedstock agnostic, meaning the CNC product quality is not substantially biomass source dependent. The biomass is almost always heavily bleached before CNC production; therefore, lignin and hemicelluloses are removed (unless they will add value, for example, with lignin increasing CNC hydrophobicity), making the exact cellulose source irrelevant (within reason; see TABLE 2). While softwood and hardwood pulps are common starting materials in industry, woodchips, bark, agricultural residues (corn cobs and stover, kenaf and cane straw), energy crops (switchgrass, miscanthus and bamboo) and purer celluloses, such as dissolving pulp and cotton, have also been demonstrated (with the last two sources having been shown to be indistinguishable at a production scale of 2 kg per day)[10]. In most production processes, the degraded sugars can be fermented into biochemicals such as bioethanol, and removed lignin can be burned for energy (as done during chemical pulping), offering other revenue streams.

Clearly, industrial production of CNCs is on the upswing, and multiple suppliers are crucial for market growth. While information regarding the cost of CNCs is difficult to find and will change over time with the process, scale and feedstock refinement, researchers and companies are encouraged to assess the added value of CNCs in their product, the volume of CNCs required (as well as the total volume of the product) and the preferred quality (or grade) of CNCs to conclude whether their cost is reasonable. Different CNC grades are evolving, including premium grades (for food, medical, cosmetic and personal care) and performance grades

(for construction, industrial processing and environmental remediation), and materials are commercially available in spray-dried, freeze-dried and dispersion forms. Standardization efforts are under way to support turning this nanoscience into true nanotechnology[5,105–111]. While some people claim the hurdles for widespread multi-sector commercialization of CNCs stem from being stuck in a position of technology push rather than market pull, commercial products do exist and many more are close to deployment. Some companies have a focus application area (for example, Anomera Inc. in cosmetics and Blue Goose Biorefineries in cement reinforcement) but for the most part they overlap in exploring the potential of CNCs in the following applications: paints, inks, varnish and coatings; adhesives; oil and gas; food; health care, pharmaceutical and dental; cosmetics; consumer and specialty paper and board; pulp, paper and industrial processing; packaging, plastics and composites; rubbers and elastomers; components in electronics; absorbents and porous materials; textiles; cement and concrete; and water treatment.

Common challenges. Despite their positive attributes and widespread industrial production, CNCs made with sulfuric acid still have limitations. One limitation is their performance at high temperatures; although CNC thermal stability is relatively high for an organic material, increasing the thermal stability would benefit, for example, melt compounding with high melting temperature polymers, and a range of engineering fluids and separation processes. CNCs made with sulfuric acid typically begin to degrade at around 150 °C in their native acid form; however, this can be extended to approximately 300 °C by neutralizing CNCs to the sodium salt form[16,77,112]. Additionally, the 'wet' thermal stability of CNC suspensions can limit their use in aqueous high-temperature applications such as fluids for enhanced oil recovery. At temperatures as low as 110 °C, aqueous suspension properties, particularly pH, colloidal stability and rheological behaviour, begin to change[113,114].

Another area where CNC performance is lacking is in environments of high ionic strength, where electrostatic interactions are screened and van der Waals attraction dominates, leading to aggregation and sedimentation of particles. CNCs begin to associate in NaCl concentrations as low as 50 mM, which subsequently affects both the rheological behaviour and the optical and liquid crystalline properties of CNCs[15,115,116]. Lastly, the use of CNCs in hydrophobic environments, for example as reinforcing agents in polymer nanocomposites, is limited by their hydrophilicity[14]. Unmodified CNCs do not disperse well in hydrophobic polymers or non-polar solvents; therefore, their nanoscale dimensions cannot be

Table 3 | **Current and planned industrial production of CNCs**

Company	Location	Biomass sources	Production volume	CNC surface chemistry	Production route	Refs[a]
Alberta-Pacific Forest Industries Inc.	Alberta, Canada	Hardwood or softwood kraft pulp and dissolving pulp	500 kg per day	Sulfated	Sulfuric acid hydrolysis (continuous process)	102
Anomera Inc.	Ontario, Canada	Softwood pulp	30 kg per day (current); 1 tonne per day (projected 2020)	Carboxylated	Dilute hydrogen peroxide oxidation	103
Blue Goose Biorefineries Inc.	Saskatchewan, Canada	Viscose grade dissolving pulp	10 kg per day	Carboxylated	Transition metal-catalysed oxidation	104
CelluForce Inc. (can also be procured from University of Maine)	Quebec, Canada	Bleached softwood kraft pulp	1 tonne per day (since 2012)	Sulfated	Sulfuric acid hydrolysis (batch process)	–
Cellulose Lab	New Brunswick, Canada	Dissolving or commercial pulp, cotton, sisal, tunicate	10 kg per day	Sulfated (plus surface modifications)	Sulfuric acid hydrolysis (batch process)	–
GranBio (formerly American Process Inc.)	Georgia, USA (Brazilian owned)	Woodchips (eucalyptus), agricultural residues, energy crops	500 kg per day	Unmodified (plus grade containing lignin coating)	AVAP® patented process with ethanol and SO_2 (continuous process)	67,229–232
FPInnovations	Quebec, Canada	Bleached chemical wood pulp	1.5 kg per day	Sulfated or phosphated	Sulfuric or phosphoric acid hydrolysis (batch process)	–
InnoTech Alberta	Alberta, Canada	Various bleached hardwood or softwood pulps	2 kg per day	Sulfated	Sulfuric acid hydrolysis (batch and continuous process)	–
Melodea Ltd	Rehovot, Israel	Various bleached hardwood or softwood pulps	>10 tonnes per year (projected 2020)	Sulfated	Sulfuric acid hydrolysis (batch process)	–
USDA Forest Products Laboratory	Wisconsin, USA	Dissolving pulp	10 kg per day	Sulfated	Sulfuric acid hydrolysis (batch process)	–

CNC, cellulose nanocrystal; USDA, US Department of Agriculture. [a]Where available, references are included for patents and journal articles describing the production route; most of the information was obtained for a presentation given at the TAPPI International Conference on Nanotechnology for Renewable Materials (2019)[98] or was obtained from market reports[11,12].

exploited. These limitations have prompted researchers to study alternative production routes aimed at expanding the use of CNCs in high-temperature processes, high ionic strength environments and hydrophobic materials. The following section discusses how new production routes may improve some of these properties. Additionally, methods to reduce environmental impact, increase yield, tune nanoparticle morphology and maintain biocompatibility are presented.

Tailoring CNC performance

Reducing environmental impact. CNCs are often described as a green material which can be used to replace petrochemically derived polymers or synthetic nanoparticles. Although CNCs are generally non-toxic[9] and are produced from renewable resources, the environmental impact of their production routes has not been studied extensively[117,118]. To understand the impact of these processes, further life cycle assessments that consider all aspects of a production route to determine its overall energy and water consumption, as well as its resulting emissions, are needed. The scale of production is also important in assessing the carbon footprint and will continue to change as larger production plants are built and optimized. Industrial processes are almost always more efficient than laboratory-scale processes, and, for example, the CelluForce Inc. process recycles the sulfuric acid and separates hydrolysed carbohydrates (for fermentation and biofuel production); therefore, embracing the biorefinery concept is an obvious next step for nanocellulose producers.

While all biomass sources for CNCs are sustainable, the exact choice can have a significant impact on the outcome of a life cycle assessment. Some people argue that chemical pulps still have a non-negligible carbon footprint despite the pulp and paper industry's strides towards meeting the principles of green chemistry[119]. In one study, CNCs produced from coconut fibres and cotton were compared, and this revealed more energy and water were required to produce CNCs from coconut fibres than from cotton[117]. This result is unsurprising because most agricultural waste products have low cellulose contents and require extensive pretreatment before CNC production. If cellulose cannot be extracted from these products efficiently, the subsequent CNC production processes will not be environmentally or economically viable.

In addition to the environmental impact of the cellulose source material, the production route itself must be considered. Unfortunately, no life cycle assessments have been performed that compare CNCs produced with methods other than sulfuric acid hydrolysis. Despite this, CNF production routes have been analysed, and some insights can be drawn. A life cycle assessment of CNFs produced by chloroacetic acid etherification and TEMPO-mediated oxidation found that the latter had a lower environmental impact[120]. Likewise, the effects of two mechanical disintegration methods were studied, and it was found that homogenization was more environmentally benign than ultrasonication[120], which suggests that avoiding the use of ultrasonication in CNC production could reduce its environmental impact. Other researchers have focused on more sustainable alternatives to sulfuric acid hydrolyses. Solid organic acids, such as oxalic acid or maleic acid, are good candidates to reduce environmental impact because they can be recrystallized after hydrolysis and subsequently reused[24,121,122]. Furthermore, some methods using organic acids also propose integration of CNC and CNF production; this adds value and increases the overall process yield[121,122]. Alternative methods forego the use of acid and instead rely on high-pressure homogenization or subcritical water to produce CNCs[23,123]. Although the detailed environmental impact remains unclear, many of these methods are likely to be an improvement over mineral acid production routes.

Increasing production yield. The CNC yield from a conventional sulfuric acid hydrolysis ranges from 20% to 75% (TABLE 1) and is primarily a function of the amount of crystalline cellulose in a given biomass source. When low acid concentrations are used, disordered regions are insufficiently hydrolysed, and although the material yield (including cellulose solid residue) may be high, the CNC yield itself is low[80]. Conversely, when harsher reaction conditions are used, crystalline regions may be subject to end-wise degradation[124], in which crystallite ends are degraded to form glucose, thus reducing the overall CNC length and yield[78,80]. Despite their tendency to produce lower yields, harsh reaction conditions are often used to produce CNCs with sulfuric acid because this results in high crystallinities, clean CNC surfaces (free of oligosaccharides) and high surface charge densities[73,76,79,80]. In addition to yield losses resulting from harsh hydrolysis conditions, CNCs hydrolysed with sulfuric acid are purified by centrifugation, which results in further yield losses[20]. To increase CNC yields, researchers have investigated alternative production routes involving weaker hydrolysis reactions[21], mechanochemical procedures[58] or sonochemical procedures[30] as well as ways to minimize purification steps.

CNC yield can be increased by use of a weaker acid or a slower hydrolysis process, such as that demonstrated by an HCl vapour phase hydrolysis method[20] (TABLE 1). Phosphoric acid, for example, can be used to produce CNCs with a yield of 76–80%, which is greater than any observed yield for sulfuric acid[25]. Further increases in yield can be obtained by combining an acid hydrolysis with mechanical disintegration or ultrasonication. For example, increased yields have been shown for phosphotungstic acid combined with ball milling, oxalic acid dihydrate combined with homogenization, and sulfuric acid combined with ultrasonication[21,58,125]. In the cases of ball milling and homogenization, high yields of nanoscale CNCs were obtained by breaking apart long cellulose chains which would otherwise not be degraded by weak acids[21,58]. In the case of ultrasonication, the added energy allows acid to rapidly penetrate the cellulose structure, which results in a shorter and more even hydrolysis[125]. A similar effect was observed by combining a mild hydrochloric acid hydrolysis with hydrothermal treatments to produce high CNC yields (up to 93%)[22]. Similarly to ultrasonication, the high temperature (110 °C) allowed rapid penetration of acid into

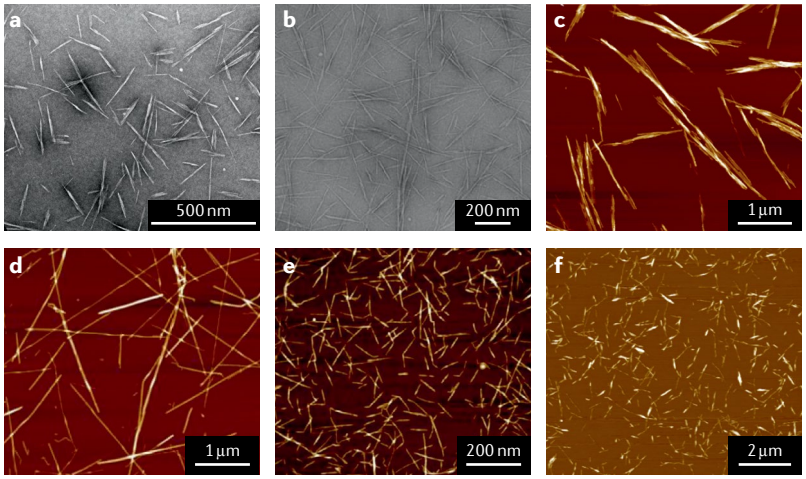

Fig. 4 | **Morphology of CNCs from various cellulose sources.** Sulfuric acid-hydrolysed cellulose nanocrystals (CNCs) from softwood bleached kraft pulp (panel **a**), sisal fibres (panel **b**), bacterial cellulose (part **c**) and tunicate cellulose (part **d**). CNCs produced by ultrasonication of (2,2,6,6-tetramethylpiperidin-1-yl)oxyl (TEMPO)-oxidized cellulose nanofibrils (panel **e**) and phosphoric acid hydrolysis of cotton (panel **f**). Panel **a** reprinted from REF.[126], Springer Nature Limited. Panel **b** reprinted from REF.[129], Springer Nature Limited. Panels **c**,**d** reprinted with permission from REF.[34], American Chemical Society. Panel **e** reprinted from REF.[30], American Chemical Society. Panel **f** reprinted with permission from REF.[57], Royal Society Publishing.

the cellulose structure[22]. Another method to increase CNC yield includes an acid-free CNC production route via extensive ultrasonication of TEMPO-oxidized wood pulp or microcrystalline cellulose[30] to produce highly charged CNCs with substantially smaller cross sections. Therefore, many methods can be used to increase CNC yields, but unfortunately, in some cases, high-yield production routes are coupled with undesirable CNC properties such as low dispersibility or colloidal stability (TABLE 1).

Tuning nanoparticle morphology. All production route parameters (for example, source material, acid or oxidizing agent, and reaction conditions) can affect CNC morphology[16,34,57]. CNCs produced from sulfuric acid typically have a whisker shape with lengths of ~100 nm and widths of 5–10 nm (FIG. 4a). It is worth noting that the microscopy technique, the measurement protocol and the bias of the researcher in particle selection all affect particle sizing results[126,127]. For example, CNCs produced from sulfuric acid hydrolysis of bleached softwood kraft pulp by CelluForce Inc. (FIG. 4a) were found to have average lengths of 84 nm and widths of 7.4 nm by TEM (more than 2,500 particles measured) and average lengths of 77 nm and heights of 3.5 nm by AFM (more than 3,000 particles measured)[126]. The discrepancy between TEM width and AFM height measurements hints at a ribbon-like CNC shape, which can be attributed to two laterally associated crystallites making up each nanoparticle[91,128]. While insights into CNC morphologies can be gained by use of both techniques, reports for CNC width or height from various research groups should not be directly compared. Current ISO efforts to standardize CNC size measurements, and interlaboratory comparisons are ongoing.

Despite the challenge of accurately quantifying dimensions, differences in morphology are still apparent for different starting cellulose sources, even when they are subjected to similar sulfuric acid hydrolyses (TABLE 2). CNCs made from sisal fibres (FIG. 4b), bacterial cellulose (FIG. 4c) and tunicates (FIG. 4d) have average lengths of 250, 1,100 and 1,200 nm, respecively, and average widths of 4, 14 and 9 nm, respectively[34,129]. Overall, cellulose starting materials with higher crystallinity, such as tunicate cellulose, produce longer nanocrystals than wood or cotton, which have more disordered cellulose regions[56,130]. The large range of CNC sizes shown in TABLE 2 is typical of nanoparticles and polymers derived from natural materials, and statistically most ranges overlap; therefore, the nanocrystal length (from common sources) can be classified only as moderately tunable.

The production route also affects CNC morphology; CNCs produced by ultrasonication of TEMPO-oxidized wood pulp have an average length of 233 nm and an average width of 3.5 nm (FIG. 4e). These CNCs have a larger aspect ratio than typical sulfated CNCs and appear more needle-like than spindle-like (that is, no tapered ends)[30]. Conversely, CNCs produced with phosphoric acid (FIG. 4f) appear larger and more end-hinged together, which can be attributed to the weaker acid hydrolysis[57].

For applications that use CNCs as viscosifying agents, a high aspect ratio CNC can reduce costs by requiring less material to achieve a given rheological profile (because of the lower overlap concentration)[131]. For example, suspensions with longer CNCs made from switchgrass have been shown to exhibit shear thinning behaviour at concentrations as low as 0.5%, while shorter CNCs made from cotton do not exhibit this behaviour until 1.5%[131]. The liquid crystalline (and optical) properties of CNCs in suspension and the ability to align CNCs using electromagnetic fields[132–134] are also highly aspect ratio dependent. Longer particles require lower concentrations to self-assemble and display shear birefringence, as well as weaker fields and less time to align[135–137]. Furthermore, the distribution of the lengths of CNCs (which depends on both the production route and the source material) as well as the twist of the CNCs themselves (which occurs along the fibril axis and is likely a function of the source material) can affect their self-assembly behaviour[87,128]. The morphology of CNCs can also affect their ability to act as strengthening agents in polymer nanocomposites[45]. CNCs with higher aspect ratios form percolating networks at lower concentrations and can subsequently provide a greater increase of the tensile modulus of a polymer than CNCs with lower aspect ratios[138]. Furthermore, CNCs with higher aspect ratios have been found to improve the crystallization of a polymer matrix[139] and to increase stress transfer from the matrix to CNCs[45,140], both of which favour nanocomposites with superior mechanical properties.

Another area in which the morphology of CNCs affects their performance is as interfacial stabilizers for Pickering emulsions, gels and foams. Longer CNCs, such as those produced from *Cladophora* algae or bacterial cellulose, form stable emulsions at lower volume fractions because single nanocrystals adsorb on several neighbouring droplets in more of a mesh-like structure. Therefore,

an interconnected and porous system of droplets can be obtained. Conversely, shorter CNCs, such as those produced from cotton, pack together more densely on droplet surfaces and stabilize individual droplets[141,142]. These are three of the most exploited value propositions of CNCs, namely rheological modification, polymer nanocomposite and cement reinforcement and interface stabilization, demonstrating that CNC morphology is crucial for material performance and product development.

Increasing thermal stability. The thermal stability of CNCs dictates their performance in formulations and materials that must be processed or used at high temperatures. Thermal stability is typically measured by thermogravimetric analysis, in which a dried cellulose sample is heated at a constant rate while its mass is monitored[143]. As mentioned, sodium-form sulfated CNCs are more stable than the corresponding acid-form CNCs[16,77], and desulfating CNCs (removing sulfate groups) can further increase their stability[112,144]. When sulfate groups are present on CNC surfaces at elevated temperatures, desulfation occurs and free sulfate ions combine with water (either bound to the CNCs or released as a by-product of degradation)[145] to produce sulfuric acid[146]. This acid further catalyses the degradation and depolymerization of cellulose chains[144]. When the sulfate groups' proton counterions are replaced with sodium ions (by the addition of sodium hydroxide), localized acid is neutralized and thermal stability is increased[16,77].

Further increases in CNC thermal stability may arise from different production routes. One example is the use of phosphoric acid to produce phosphorylated CNCs, which have higher thermal stability than sulfated CNCs[25]. The phosphate groups on CNC surfaces appear to behave very similarly to their sulfate counterparts: at high temperatures, they are hydrolysed from CNC surfaces and produce localized phosphoric acid[147,148]. Despite this, phosphorylated CNCs have significantly lower surface charge density than sulfated CNCs; therefore, less (and weaker) acid is produced and their thermal stability is higher[16]. Another contributor to the higher thermal stability of phosphorylated CNCs is the higher degree of polymerization of cellulose; this is a direct result of the weaker acid hydrolysis. CNCs with longer cellulose chains have fewer reducing ends per mass of cellulose; this increases their thermal stability because reducing ends are known to activate cellulose pyrolysis[149]. While many postproduction surface modification routes[69] can also increase thermal stability, end-specific modification of CNCs[150] may be particularly promising as this could protect cellulose chain reducing ends from thermally induced depolymerization or end-specific polymer grafting could give CNCs a larger degree of polymerization. Therefore, CNCs produced in less harsh reaction conditions (shorter reaction time, lower temperature or weaker acid) are generally more thermally stable because they have fewer surface charge groups and longer cellulose chains[16,77].

While the effect of surface charge density on thermal stability is fairly clear, the effect of surface chemistry remains less obvious. CNCs hydrolysed with organic acids are perceived to be more thermally stable than CNCs hydrolysed with mineral acids[24,29,151] but the root cause is not well understood. The morphology, crystallinity and colloidal stability of CNCs made with organic acids are different from those of CNCs made with sulfuric acid (TABLE 1). In addition to having different surface chemistries, the cellulose chains have a different degree of polymerization and degree of order, which affects their thermal stability. Furthermore, the thermal stability of CNCs made with organic acids is often compared with that of CNCs made with sulfuric acid in acid form (their least stable form). As a result, it is difficult to draw conclusions from the literature particularly when thermal stability is compared between laboratories where sample preparation, instruments and standard operating procedures differ[143]. Overall, however, the increased thermal stability of CNCs made with organic acids follows the trend discussed earlier: CNCs subjected to weaker hydrolysis procedures are generally more thermally stable.

Tailoring hydrophilicity. CNCs have strong affinity for water owing to abundant surface hydroxy groups; they bind water[152] but do not dissolve in it[153,154], and newer results suggest that some water may go into microfibril aggregates, which could lead to slight nanocrystal swelling[155,156]. For the most part, however, CNCs forming strong hydrogen bonds with water is an advantage: dried CNCs can be redispersed in water (with some energy input, for example, ultrasonication) to form stable aqueous suspensions[101,157] — this is not the case for most other nanoparticles[158]. When CNCs are dried, the cohesion between particles is primarily attributed to van der Waals forces and CNC–CNC hydrogen bonds[152,159] but the hydrogen bonds are easily replaced with CNC–solvent hydrogen bonds when the CNCs are wetted with water or highly polar liquids such as dimethyl sulfoxide, dimethylformamide and formic acid[7,159,160]. The crystalline structure of cellulose, however, does not support an entirely hydrophilic material because individual cellulose chains are ordered in such a way that the crystal structure contains planes which are rich in hydroxy groups and others which are void of them[142]. The planes void of hydroxy groups are referred to as the 'hydrophobic edges' because they are not as prone to hydrogen bonding as the other crystal planes[161]. While nanoparticles are thermodynamically driven to interfaces unless they have extremely low or high water contact angles, intermediate wettability combined with this somewhat amphiphilic behaviour of CNCs from their crystal structure is advantageous in stabilizing oil–water interfaces; for example, as Pickering emulsion stabilizers[142]. For some applications, however, the propensity of CNCs to hydrogen bond presents a significant challenge, one that cannot be overcome by the presence of a hydrophobic edge. This challenge is particularly relevant in polymer nanocomposites, where CNCs are ideal reinforcing agents; however, their use is limited by their incompatibility with hydrophobic solvents and polymers.

To increase compatibility between CNCs and hydrophobic solvents and polymers, CNCs can be functionalized after production by small-molecule modifications and polymer grafting, as reviewed extensively[14,69].

Polymer grafting has tuned the hydrophilicity of CNCs up to contact angles as high as 130° (REFS[162,163]) but unfortunately these procedures tend to require many steps, expensive solvents and extensive purification, all of which result in a costly product with limited industrial relevance[14]. Therefore, there is a need for direct modification of CNC surface chemistry and hydrophobicity during production. Tuning the functionality of CNCs in situ can be done, for example, in a mixed acid hydrolysis by combining hydrochloric acid with either acetic acid or butyric acid, thus producing CNCs with acetate or butyrate groups, respectively[164]. The acetate-bearing and butyrate-bearing CNCs demonstrated higher contact angles than unmodified CNCs (made with hydrochloric acid only) as well as improved dispersibility in toluene. Similarly, ionic liquids with acetate functionalities have been used to produce less hydrophilic CNCs by acetylating the surface hydroxy groups. CNCs produced in one-pot methods with either 1-ethyl-3-methylimidazolium acetate[35] or tetrabutylammonium acetate[37] have contact angles of 52° and 55°, respectively (compared with approximately 20° for unmodified sulfated CNCs).

Despite increases in their compatibility with hydrophobic matrices, the CNCs produced by the methods mentioned above have low colloidal stability and form large aggregates in aqueous suspensions. To produce less hydrophilic CNCs that still meet the target properties discussed in previous sections, conventional hydrolysis methods can be used on unconventional sources. Lignin-rich biomass such as unbleached pulps, fibres or fine fractions can be used to produce lignin-containing CNCs[39,122,165,166]. Conversely, GranBio produces lignin-coated CNCs by precipitating lignin onto the nanocellulose surfaces[67]. Films made from lignin-containing CNCs and lignin-coated CNCs have contact angles of 69° and 50°, respectively[166] but are still fairly dispersible in water. Additionally, the morphologies of these CNCs are similar to those of CNCs from wood or cotton. Therefore, although the results are not as dramatic as those obtained via polymer grafting routes, in situ methods can be used to increase compatibility of CNCs with hydrophobic systems.

The last category of routes to control CNC compatibility includes producing CNCs with surface chemistries that reduce the number of steps (and associated purification) needed to add further functionality, therefore making the CNCs one step closer to the desired end product. Countless studies in the literature used the more conventional sulfated CNCs with a postproduction TEMPO-mediated oxidation [167,168] or periodate oxidation[169] to add carboxyl groups to CNC surfaces[170]. Directly carboxylated CNCs can save time and effort; oxidative and organic acid hydrolysis methods lead to CNCs that can be made hydrophobic, cationic, conductive, antibacterial and polymer brush coated with only one additional step (for example, using carbodiimide coupling). Similarly, CNCs produced with a combination of hydrochloric acid and 2-bromopropionic acid have Br surface groups suitable for initiating atom transfer radical polymerization (that is, controlled polymer grafting from CNCs), saving the initiator immobilization step, which has low efficiency and is cumbersome[14,171]. Note that hydrobromic acid hydrolysis does not impart Br surface groups in this way[26]. Changing the surface chemistry and charge density has also been demonstrated to affect nanoparticle nucleation and binding (with inorganic nanoparticles, metal–organic frameworks, graphene and quantum dots) as another route to enhance CNC functionality[172–175]. Likely, the industrial feasibility of multistep surface modification routes for CNCs needs to be evaluated on a case-by-case basis and strongly depends on the value added (such as new bioactive, catalytic, sorptive or optical features); however, the production route should be considered, given the large range of surface functionalities achievable (TABLE 1).

Imparting steric stability. CNCs typically have anionic surface moieties; therefore, they maintain colloidal stability on the basis of DLVO theory. When subjected to sodium chloride concentrations as low as 0.05 M (REF.[15]), CNCs aggregate and sediment owing to compression of the electrostatic double layer. To overcome this challenge, CNCs can be sterically or electrosterically stabilized, which was first accomplished by Araki et al. by grafting amino-terminated poly(ethylene glycol) to carboxylated CNCs[64]. The resulting CNCs maintained their colloidal stability in a 2 M NaCl solution[64]. A similar resistance to aggregation in high ionic strength environments was shown by Azzam et al.[176] and in one step less by Kloser and Grey[177]. As discussed earlier, most methods require multiple steps and are not cost-effective, motivating the production of sterically stabilized CNCs via in situ methods. To date, a range of periodate oxidation methods (performed on wood pulp and microfibrillated cellulose) exist to produce hairy CNCs, which are sterically stabilized by amorphous dialdehyde cellulose chains[41,178] or reduced dangling polyol chains[66]. Additionally, these hairy CNCs can be further oxidized via chlorite oxidation or TEMPO-mediated oxidation to yield electrosterically stabilized CNCs[179,180]. The morphology is similar to that of acid-hydrolysed CNCs; hairy dialdehyde CNCs have lengths ranging from 120 to 200 nm and widths of approximately 13 nm (by AFM)[180], while polyol-stabilized CNCs have average lengths of 54–67 nm and widths of 6.1–6.5 nm (by TEM)[66]. Their most interesting property, however, is their ability to resist aggregation at high salt concentrations: the hydrodynamic diameters (as measured by DLS) of dialdehyde and polyol CNCs were constant in sodium chloride up to 2 M and 1 M, respectively[66,180]. Furthermore, the long dialdehyde cellulose chains which extend from the surfaces of these CNCs allows their use as bridging flocculants[181,182]. Overall, this novel CNC production route is an alternative to complex polymer grafting steps for sterically or electrosterically stabilizing CNCs, indicating that moderate control of steric stabilization potential is possible by adjustment of the CNC production route.

Maintaining biocompatibility. CNCs have potential for many biomedical applications, including medical implants, drug delivery and tissue engineering[183], all of which require them to be biocompatible, non-toxic and not accumulate in the body. CNCs do not break down

Table 4 | **The tunability and importance of cellulose nanocrystal properties in four application areas**

Property	Tunability through production route	Importance			
		Biomedical devices	Nanocomposites	Rheological modifiers	Emulsions and foams
Aspect ratio	Medium	–	+++	+++	++
Surface charge density	High	++	–	+	+++
Surface chemistry	High	+++	+	–	–
Wettability	Low	+	+++	++	++
Thermal stability	Medium	–	++	+	–
Individualized particles (non-aggregated)	Low	++	++	–	+
Crystallinity	Low	–	+++	–	–
Stability in high ionic strength environments	Medium	+	–	++	+

The properties are rated by importance: +, slightly important; ++, moderately important; +++, highly important.

in vivo; however, they can be designed into materials that are resorbable, whereby the tethers between particles degrade predictably and the CNCs are cleared by normal clearance pathways[184,185]. CNC properties such as surface chemistry, surface charge density, hydrophilicity, size and aspect ratio can affect their biocompatibility and cytotoxicity[183,186,187]. While CNCs are generally perceived to be non-toxic[9,185,188], some studies indicate otherwise[187]. CNCs which are larger or more aggregated have shown higher cytotoxicity than smaller CNCs, particularly at high concentrations. This increased cytotoxicity could be a result of CNC aggregation or gelation around cell membranes, which would prevent gas exchange[189]. Similarly, CNCs with different morphologies and degrees of aggregation, despite being from the same source material, were found to elicit different pulmonary responses in mice[186]. In addition to CNC morphology, surface charge density and surface chemistry play an important role in determining biocompatibility. In mammalian cells, mitochondrial activity was found to decrease with increasing surface charge density of carboxylated CNCs[190]. However, the in vivo response of a CNC type cannot be predicted; its compatibility and cytotoxicity must be assessed, and overall, long-term studies are lacking. As discussed in the preceding sections, CNC samples can be unique, and different combinations of morphology, surface chemistry (or other components in the mixture), surface charge density and crystallinity can have surprising effects on biological viability.

Outlook

This Review has summarized numerous routes to produce CNCs and evaluated the outputs according to target properties. Traditional CNCs, made by sulfuric acid hydrolysis of wood or cotton, have high colloidal stability in water, a nanoscale rod shape and a high degree of crystallinity. Additionally, they are produced industrially by a relatively green process as a uniform, high-quality nanomaterial in tonne-per-day quantities; therefore, they are suitable for a broad range of applications. In this section, we highlight four promising application areas for CNCs: materials for biomedical devices; reinforcing agents in nanocomposites; rheological modifiers; and interfacial stabilizers for emulsions, gels and foams (TABLE 4).

Another long-discussed application of CNCs is in optical materials, which can be made by exploiting their tendency to self-assemble into chiral nematic liquid crystals. Despite extensive publications[191,192] and patents[193,194] demonstrating proof of concept as optical filters, biodegradable pigments, anticounterfeiting components in security paper, chiral separators, sensors and iridescent coatings, many challenges exist in the scale-up of these materials. Primarily, they require slow drying of water from concentrated CNC suspensions, the optical properties are highly sensitive to additives, impurities and drying conditions, and the resulting materials tend to be multidomained in texture; that is, they do not show perfect long-range orientation, which may be required for some applications. As a result, we have not included optical materials in the emerging applications discussed in this section.

For the remaining applications, the aforementioned target properties are essential; well-dispersed, nanowhisker-shaped particles with crystalline morphology contribute to material performance. However, the performance can be further improved by selecting CNCs that meet additional criteria, such as high thermal stability, high aspect ratio and colloidal stability in aqueous environments of high ionic strength. The potential to expand the use of CNCs and improve material behaviour has motivated researchers to investigate alternative source materials and production routes, which may also increase yield and economics, and limit further physical and chemical CNC treatments down the line. In some cases, the new CNCs produced fail to achieve the basic target properties; this simply demonstrates the magnitude of the challenge. In other cases, new production routes show promise, and we offer our perspective on how to select the right CNC for the job in the following subsections.

Biomedical devices. For biomedical devices (for example, drug delivery, tissue regeneration, cell culturing platforms, bioadhesives, biosensors, probes and membranes) biocompatibility is the most important factor in determining the feasibility of incorporating CNCs.

CNC users in this field should seek out nanoparticles which have compatible surface chemistry, relatively low surface charge density (threshold values depend on surface chemistry) and (generally) small dimensions. CNCs made with strong acids are a suitable option: a high acid concentration (which leads to smaller CNCs) can be used; however, the effects of surface charge density and surface chemistry on cytotoxicity with regard to targeted cells will have to be carefully evaluated. We also note that most electrostatically stabilized CNCs become colloidally unstable under physiological conditions of high ionic strength, suggesting that aggregation should also be investigated as it would affect cell uptake and toxicity; sterically stabilized CNCs may offer a particular advantage in such applications. Production routes that lead to an abundance of aldehyde surface moieties (for example, sodium periodate methods), cationic surface charges or CNCs that are not pure cellulose (for example, that contain significant lignin or hemicellulose) should be avoided owing to their inherent cytotoxicity. The ability to produce fully purified and reproducible CNCs may be the most crucial in this category, again suggesting that strong acid hydrolysis routes are ideal.

Nanocomposites. CNCs also show great potential as additives in nanocomposites (where the matrix is, for example, a thermoplastic or thermoset polymer, hydrogel, cement, concrete, ceramic or latex); however, the greatest barrier in this category is CNC hydrophilicity. Nanocomposites that can be processed in water, such as water-soluble polymers, cements and latexes, therefore have significant advantages and are straightforward with unmodified CNCs, as long as the CNCs are well dispersed to begin with. For melt-compounding polymer nanocomposites, high thermal stability of CNCs is paramount. In all cases, higher aspect ratios are desirable for better mechanical improvement at lower loadings. Therefore, for CNC users targeting nanocomposite applications, highly crystalline source materials that give longer CNCs, in situ grafting routes, hydrophobically coated CNCs (for example, lignin) or organic acid hydrolyses can be used. Furthermore, if high-temperature processing is required, low charge density, high cellulose degree of polymerization, non-sulfated surface chemistry and appropriate selection of the CNC counterion can help.

Rheological modifiers. For CNCs as rheological modifiers in industrial fluids (for example, oil and gas extraction and processing fluids), cosmetics, food, paints, lubricants and household formulated products, suspension stability, or controlled aggregation, is essential. Fortunately, many of these products are water based and inherently compatible with cellulose. However, the end user must consider all components of a formulation, how they will interact with CNCs, under what conditions they will be used and for how long the suspension properties need to be consistent. For high ionic strength environments, steric stabilization is beneficial and can be achieved via sodium periodate oxidation. For dilute liquid formulated products, choosing a CNC with high surface charge density (from sulfuric acid, oxalic acid or maleic acid hydrolysis or TEMPO or H_2O_2 oxidation) is recommended, although desulfation will occur over time and is accelerated with heating[146], suggesting a slight preference for carboxylated CNCs. Finally, the propensity of CNCs to interact strongly with water and their aspect ratio are important factors. Therefore, CNCs with cleaner surfaces (from harsher hydrolyses) bind more water[79] and CNCs with higher aspect ratios form higher-viscosity suspensions at lower concentrations.

Emulsion, gels and foams. CNCs are promising as interfacial stabilizers in emulsions, gels and foams (again for cosmetic, food, pharmaceutical, latex, industrial processing and formulated household product applications). The surface charge density strongly affects the performance of CNCs in emulsions and foams; therefore, less harsh production routes (such as weaker acids) can be used to reduce surface charge density and allow denser packing of CNCs at interfaces, which imparts increased stability. However, some surface charge promotes electrostatic repulsion between droplets, offering more resistance to coalescence (in addition to the steric barriers provided by the nanoparticles). Another influential property for this application is the aspect ratio of the CNCs, which can partially be used to tune the size and type of droplets that form in CNC-stabilized emulsions and aqueous foams and control the rheology of the continuous phase, which also increases stability. Lastly, the wettability of CNCs can be tuned by changing the source material (lignin-rich sources are less hydrophilic) or by covalent or adsorption-based surface functionalization methods, consequently affecting their behaviour at interfaces.

Looking ahead. Overall, these four application areas demonstrate the versatility of CNCs and their ability to add value to a wide range of products. This includes both improving currently known materials with CNCs (nano-enhanced) and the design of entirely new materials for the future that will be possible only because of CNCs (nano-enabled). Successfully incorporating CNCs into hybrid, composite and formulated products, however, requires careful consideration of the material and its intended use. While CNCs produced with sulfuric acid are the most commercially available and most widely used (as well as the most uniform and most reproducible in properties), they may not be the optimal choice for every application. To optimize the performance of materials that incorporate CNCs, researchers must select CNCs with suitable surface chemistry, surface charge density, crystallinity and aspect ratio, as each target application requires a different set of CNC properties. Often, some properties must be compromised to achieve others. Furthermore, researchers and developers may face additional challenges in the use of CNCs from alternative production routes because many have not been scaled up and are therefore not currently suitable for high-volume applications. Therefore, to continue expanding the use of CNCs in commercial products, economically feasible, large-scale processes offering a wide range of properties are essential.

Published online: 13 October 2020

1. Nickerson, R. F. & Habrle, J. A. Cellulose intercrystalline structure. *Ind. Eng. Chem.* **39**, 1507–1512 (1947).
2. Rånby, B. G., Banderet, A. & Sillén, L. G. Aqueous colloidal solutions of cellulose micelles. *Acta Chem. Scand.* **3**, 649–650 (1949).
3. Rånby, B. G. The colloidal properties of cellulose micelles. *Discuss. Faraday Soc.* **11**, 158–164 (1951).
4. Mukherjee, S. M. & Woods, H. J. X-ray and electron microscope studies of the degradation of cellulose by sulphuric acid. *Biochim. Biophys. Acta* **10**, 499–511 (1953).
5. International Organization for Standardization. Nanotechnologies — standard terms and their definition for cellulose nanomaterial ISO/TS 20477 (IOS, 2017).
6. Tashiro, K. & Kobayashi, M. Theoretical evaluation of three-dimensional elastic constants of native and regenerated celluloses: role of hydrogen bonds. *Polymer* **32**, 1516–1526 (1991).
7. Viet, D., Beck-Candanedo, S. & Gray, D. G. Dispersion of cellulose nanocrystals in polar organic solvents. *Cellulose* **14**, 109–113 (2007).
8. Revol, J.-F., Bradford, H., Giasson, J., Marchessault, R. H. & Gray, D. G. Helicoidal self-ordering of cellulose microfibrils in aqueous suspension. *Int. J. Biol. Macromol.* **14**, 170–172 (1992).
9. Roman, M. Toxicity of cellulose nanocrystals: a review. *Ind. Biotechnol.* **11**, 25–33 (2015).
10. Reid, M. S., Villalobos, M. & Cranston, E. D. Benchmarking cellulose nanocrystals: from the laboratory to industrial production. *Langmuir* **33**, 1583–1598 (2017).
11. Miller, J. *Nanocellulose: Producers, Products, and Applications* (TAPPI, 2017).
12. Research and Markets. The global market for nanocellulose. *Research and Markets* https://www.researchandmarkets.com/reports/4827614/the-global-market-for-nanocellulose?utm_code=bcb85m&utm_medium=BW (2019).
13. Lu, P. & Hsieh, Y. L. O. Preparation and properties of cellulose nanocrystals: Rods, spheres, and network. *Carbohydr. Polym.* **82**, 329–336 (2010).
14. Kedzior, S. A., Zoppe, J. O., Berry, R. M. & Cranston, E. D. Recent advances and an industrial perspective of cellulose nanocrystal functionalization through polymer grafting. *Curr. Opin. Solid State Mater. Sci.* **23**, 74–91 (2019).
15. Cherhal, F., Cousin, F. & Capron, I. Influence of charge density and ionic strength on the aggregation process of cellulose nanocrystals in aqueous suspension, as revealed by small-angle neutron scattering. *Langmuir* **31**, 5596–5602 (2015).
16. Vanderfleet, O. M. et al. Insight into thermal stability of cellulose nanocrystals from new hydrolysis methods with acid blends. *Cellulose* **26**, 507–528 (2019).
17. Teixeira, E. et al. Sugarcane bagasse whiskers: extraction and characterizations. *Ind. Crop. Prod.* **33**, 63–66 (2011).
18. Bano, S. & Negi, Y. S. Studies on cellulose nanocrystals isolated from groundnut shells. *Carbohydr. Polym.* **157**, 1041–1049 (2017).
19. Melikog˘lu, A. Y., Bilek, S. E. & Cesur, S. Optimum alkaline treatment parameters for the extraction of cellulose and production of cellulose nanocrystals from apple pomace. *Carbohydr. Polym.* **215**, 330–337 (2019).
20. Kontturi, E. et al. Degradation and crystallization of cellulose in hydrogen chloride vapor for high-yield isolation of cellulose nanocrystals. *Angew. Chem. Int. Ed.* **55**, 14455–14458 (2016).
21. Lu, Q. et al. Extraction of cellulose nanocrystals with a high yield of 88% by simultaneous mechanochemical activation and phosphotungstic acid hydrolysis. *ACS Sustain. Chem. Eng.* **4**, 2165–2172 (2016).
22. Yu, H. et al. Facile extraction of thermally stable cellulose nanocrystals with a high yield of 93% through hydrochloric acid hydrolysis under hydrothermal conditions. *J. Mater. Chem. A* **1**, 3938–3944 (2013).
23. Novo, L. P., Bras, J., García, A., Belgacem, N. & Curvelo, A. A. S. Subcritical water: a method for green production of cellulose nanocrystals. *ACS Sustain. Chem. Eng.* **3**, 2839–2846 (2015).
24. Chen, L. et al. Highly thermal-stable and functional cellulose nanocrystals and nanofibrils produced using fully recyclable organic acids. *Green. Chem.* **18**, 3835–3843 (2016).
25. Camarero Espinosa, S. et al. Isolation of thermally stable cellulose nanocrystals by phosphoric acid hydrolysis. *Biomacromolecules* **14**, 1223–1230 (2013).
26. Sadeghifar, H., Filpponen, I., Clarke, S. P., Brougham, D. F. & Argyropoulos, D. S. Production of cellulose nanocrystals using hydrobromic acid and click reactions on their surface. *J. Mater. Sci.* **46**, 7344–7355 (2011).
27. Li, D., Henschen, J. & Ek, M. Esterification and hydrolysis of cellulose using oxalic acid dihydrate in a solvent-free reaction suitable for preparation of surface-functionalised cellulose nanocrystals with high yield. *Green Chem.* **19**, 5564–5567 (2017).
28. Boujemaoui, A., Mongkhontreerat, S., Malmström, E. & Carlmark, A. Preparation and characterization of functionalized cellulose nanocrystals. *Carbohydr. Polym.* **115**, 457–464 (2015).
29. Yu, H.-Y., Zhang, D.-Z., Lu, F.-F. & Yao, J. New approach for single-step extraction of carboxylated cellulose nanocrystals for their use as adsorbents and flocculants. *ACS Sustain. Chem. Eng.* **4**, 2632–2643 (2016).
30. Zhou, Y., Saito, T., Bergström, L. & Isogai, A. Acid-free preparation of cellulose nanocrystals by TEMPO oxidation and subsequent cavitation. *Biomacromolecules* **19**, 633–639 (2018).
31. Leung, A. C. W. et al. Characteristics and properties of carboxylated cellulose nanocrystals prepared from a novel one-step procedure. *Small* **7**, 302–305 (2011).
32. Filson, P. B., Dawson-Andoh, B. E. & Schwegler-Berry, D. Enzymatic-mediated production of cellulose nanocrystals from recycled pulp. *Green Chem.* **11**, 1808–1814 (2009).
33. Siqueira, G., Tapin-Lingua, S., Bras, J., da Silva Perez, D. & Dufresne, A. Morphological investigation of nanoparticles obtained from combined mechanical shearing, and enzymatic and acid hydrolysis of sisal fibers. *Cellulose* **17**, 1147–1158 (2010).
34. Sacui, I. A. et al. Comparison of the properties of cellulose nanocrystals and cellulose nanofibrils isolated from bacteria, tunicate, and wood processed using acid, enzymatic, mechanical, and oxidative methods. *ACS Appl. Mater. Interfaces* **6**, 6127–6138 (2014).
35. Abushammala, H., Krossing, I. & Laborie, M. P. Ionic liquid-mediated technology to produce cellulose nanocrystals directly from wood. *Carbohydr. Polym.* **134**, 609–616 (2015).
36. Man, Z. et al. Preparation of cellulose nanocrystals using an ionic liquid. *J. Polym. Environ.* **19**, 726–731 (2011).
37. Miao, J., Yu, Y., Jiang, Z. & Zhang, L. One-pot preparation of hydrophobic cellulose nanocrystals in an ionic liquid. *Cellulose* **23**, 1209–1219 (2016).
38. Sirviö, J. A., Visanko, M. & Liimatainen, H. Acidic deep eutectic solvents as hydrolytic media for cellulose nanocrystal production. *Biomacromolecules* **17**, 3025–3032 (2016).
39. Jiang, J. et al. High production yield and more thermally stable lignin-containing cellulose nanocrystals isolated using a ternary acidic deep eutectic solvent. *ACS Sustain. Chem. Eng.* **8**, 7182–7191 (2020).
40. Trache, D., Hussin, M. H., Haafiz, M. K. M. & Thakur, V. K. Recent progress in cellulose nanocrystals: sources and production. *Nanoscale* **9**, 1763–1786 (2017).
41. Van De Ven, T. G. M. & Sheikhi, A. Hairy cellulose nanocrystalloids: a novel class of nanocellulose. *Nanoscale* **8**, 15101–15114 (2016).
42. Lin, K.-H. et al. An analysis on the electrophoretic mobility of cellulose nanocrystals as thin cylinders: relaxation and end effect. *RSC Adv.* **9**, 34032–34038 (2019).
43. Bhattacharjee, S. DLS and zeta potential - what they are and what they are not? *J. Control. Rel.* **235**, 337–351 (2016).
44. Foster, E. J. et al. Current characterization methods for cellulose nanomaterials. *Chem. Soc. Rev.* **47**, 2609–2679 (2018).
45. Eichhorn, S. J. et al. Review: current international research into cellulose nanofibres and nanocomposites. *J. Mater. Sci.* **45**, 1–33 (2010).
46. Phan-Xuan, T. et al. Aggregation behavior of aqueous cellulose nanocrystals: the effect of inorganic salts. *Cellulose* **23**, 3653–3663 (2016).
47. Fraschini, C. et al. Critical discussion of light scattering and microscopy techniques for CNC particle sizing. *Nord. Pulp Pap. Res. J.* **29**, 31–40 (2014).
48. Boluk, Y. & Danumah, C. Analysis of cellulose nanocrystal rod lengths by dynamic light scattering and electron microscopy. *J. Nanopart. Res.* **16**, 2174 (2014).
49. Ogawa, Y. & Putaux, J. L. Transmission electron microscopy of cellulose. Part 2: technical and practical aspects. *Cellulose* **26**, 17–34 (2019).
50. Sèbe, G., Ham-Pichavant, F., Ibarboure, E., Koffi, A. L. C. & Tingaut, P. Supramolecular structure characterization of cellulose II nanowhiskers produced by acid hydrolysis of cellulose I substrates. *Biomacromolecules* **13**, 570–578 (2012).
51. Yue, Y. et al. Comparative properties of cellulose nano-crystals from native and mercerized cotton fibers. *Cellulose* **19**, 1173–1187 (2012).
52. Agarwal, U. P., Ralph, S. A., Reiner, R. S. & Baez, C. Probing crystallinity of never-dried wood cellulose with Raman spectroscopy. *Cellulose* **23**, 125–144 (2016).
53. Park, S., Baker, J. O., Himmel, M. E., Parilla, P. A. & Johnson, D. K. Cellulose crystallinity index: Measurement techniques and their impact on interpreting cellulase performance. *Biotechnol. Biofuels* **3**, 1–10 (2010).
54. Segal, L., Creely, J. J., Martin, A. E. & Conrad, C. M. An empirical method for estimating the degree of crystallinity of native cellulose using the X-ray diffractometer. *Text. Res. J.* **29**, 786–794 (1959).
55. Xiang, Q., Lee, Y. Y., Pettersson, P. O. & Torget, R. W. in *Applied Biochemistry and Biotechnology* (eds Davison, B. H., Lee, J. W., Finkelstein, M. & McMillan, J. D.) 505–514 (Humana Press, 2003).
56. Battista, O. A., Coppick, S., Howsmon, J. A., Morehead, F. F. & Sisson, W. A. Level-off degree of polymerization. *Ind. Eng. Chem.* **48**, 333–335 (1956).
57. Vanderfleet, O. M., Osorio, D. A. & Cranston, E. D. Optimization of cellulose nanocrystal length and surface charge density through phosphoric acid hydrolysis. *Phil. Trans. R. Soc. A* **376**, 1–7 (2018).
58. Henschen, J., Li, D. & Ek, M. Preparation of cellulose nanomaterials via cellulose oxalates. *Carbohydr. Polym.* **213**, 208–216 (2019).
59. Bian, H., Chen, L., Dai, H. & Zhu, J. Y. Effect of fiber drying on properties of lignin containing cellulose nanocrystals and nanofibrils produced through maleic acid hydrolysis. *Cellulose* **24**, 4205–4216 (2017).
60. Du, H. et al. Preparation and characterization of thermally stable cellulose nanocrystals via a sustainable approach of $FeCl_3$-catalyzed formic acid hydrolysis. *Cellulose* **23**, 2389–2407 (2016).
61. Castro-Guerrero, C. F. & Gray, D. G. Chiral nematic phase formation by aqueous suspensions of cellulose nanocrystals prepared by oxidation with ammonium persulfate. *Cellulose* **21**, 2567–2577 (2014).
62. Montanari, S., Roumani, M., Heux, L. & Vignon, M. R. Topochemistry of carboxylated cellulose nanocrystals resulting from TEMPO-mediated oxidation. *Macromolecules* **38**, 1665–1671 (2005).
63. Habibi, Y., Chanzy, H. & Vignon, M. R. TEMPO-mediated surface oxidation of cellulose whiskers. *Cellulose* **13**, 679–687 (2006).
64. Araki, J., Wada, M. & Kuga, S. Steric stabilization of a cellulose microcrystal suspension by poly(ethylene glycol) grafting. *Langmuir* **17**, 21–27 (2001).
65. Salajková, M., Berglund, L. A. & Zhou, Q. Hydrophobic cellulose nanocrystals modified with quaternary ammonium salts. *J. Mater. Chem.* **22**, 19798–19805 (2012).
66. Leguy, J. et al. Periodate oxidation followed by $NaBH_4$ reduction converts microfibrillated cellulose into sterically stabilized neutral cellulose nanocrystal suspensions. *Langmuir* **34**, 11066–11075 (2018).
67. Nelson, K. & Retsina, T. Innovative nanocellulose process breaks the cost barrier. *TAPPI J.* **13**, 19–23 (2014).
68. Wu, B., Wang, S., Tang, J. & Lin, N. in *Advanced Functional Materials from Nanopolysaccharides* (eds Lin, N., Tang, J., Dufresne, A. & Tam, M. K. C.) 389–409 (Springer, 2019).
69. Habibi, Y. Key advances in the chemical modification of nanocelluloses. *Chem. Soc. Rev.* **43**, 1519–1542 (2014).
70. Tan, X. Y., Abd Hamid, S. B. & Lai, C. W. Preparation of high crystallinity cellulose nanocrystals (CNCs) by ionic liquid solvolysis. *Biomass Bioenergy* **81**, 584–591 (2015).
71. Filson, P. B. & Dawson-Andoh, B. E. Sono-chemical preparation of cellulose nanocrystals from lignocellulose derived materials. *Bioresour. Technol.* **100**, 2259–2264 (2009).
72. Dong, S., Bortner, M. J. & Roman, M. Analysis of the sulfuric acid hydrolysis of wood pulp for cellulose nanocrystal production: a central composite design study. *Ind. Crop. Prod.* **93**, 1–12 (2016).
73. Bondeson, D., Mathew, A. & Oksman, K. Optimization of the isolation of nanocrystals from microcrystalline cellulose by acid hydrolysis. *Cellulose* **13**, 171–180 (2006).
74. Dong, X. M., Revol, J.-F. & Gray, D. G. Effect of microcrystallite preparation conditions on the formation of colloid crystals of cellulose. *Cellulose* **5**, 19–32 (1998).

75. Beck-Candanedo, S., Roman, M. & Gray, D. G. Effect of reaction conditions on the properties and behavior of wood cellulose nanocrystal suspensions. *Biomacromolecules* **6**, 1048–1054 (2005).
76. Hamad, W. Y. & Hu, T. Q. Structure-process-yield interrelations in nanocrystalline cellulose extraction. *Can. J. Chem. Eng.* **88**, 392–402 (2010).
77. Kargarzadeh, H. et al. Effects of hydrolysis conditions on the morphology, crystallinity, and thermal stability of cellulose nanocrystals extracted from kenaf bast fibers. *Cellulose* **19**, 855–866 (2012).
78. Wang, Q., Zhao, X. & Zhu, J. Y. Kinetics of strong acid hydrolysis of a bleached kraft pulp for producing cellulose nanocrystals (CNCs). *Ind. Eng. Chem. Res.* **53**, 11007–11014 (2014).
79. Bouchard, J., Méthot, M., Fraschini, C. & Beck, S. Effect of oligosaccharide deposition on the surface of cellulose nanocrystals as a function of acid hydrolysis temperature. *Cellulose* **23**, 3555–3567 (2016).
80. Chen, L. et al. Tailoring the yield and characteristics of wood cellulose nanocrystals (CNC) using concentrated acid hydrolysis. *Cellulose* **22**, 1753–1762 (2015).
81. Novo, L. P. et al. A study of the production of cellulose nanocrystals through subcritical water hydrolysis. *Ind. Crop. Prod.* **93**, 88–95 (2016).
82. Hemmati, F., Jafari, S. M., Kashaninejad, M. & Barani Motlagh, M. Synthesis and characterization of cellulose nanocrystals derived from walnut shell agricultural residues. *Int. J. Biol. Macromol.* **120**, 1216–1224 (2018).
83. Prasad Reddy, J. & Rhim, J. W. Isolation and characterization of cellulose nanocrystals from garlic skin. *Mater. Lett.* **129**, 20–23 (2014).
84. Santos, R. M. dos et al. Cellulose nanocrystals from pineapple leaf, a new approach for the reuse of this agro-waste. *Ind. Crop. Prod.* **50**, 707–714 (2013).
85. Jiang, F. & Hsieh, Y. L. O. Cellulose nanocrystal isolation from tomato peels and assembled nanofibers. *Carbohydr. Polym.* **122**, 60–68 (2015).
86. Johar, N., Ahmad, I. & Dufresne, A. Extraction, preparation and characterization of cellulose fibres and nanocrystals from rice husk. *Ind. Crop. Prod.* **37**, 93–99 (2012).
87. Schütz, C. et al. Effect of source on the properties and behavior of cellulose nanocrystal suspensions. *ACS Sustain. Chem. Eng.* **6**, 8317–8324 (2018).
88. Nishiyama, Y. et al. Periodic disorder along ramie cellulose microfibrils. *Biomacromolecules* **4**, 1013–1017 (2003).
89. Cudjoe, E. et al. Miscanthus giganteus: a commercially viable sustainable source of cellulose nanocrystals. *Carbohydr. Polym.* **155**, 230–241 (2017).
90. Cao, X., Ding, B., Yu, J. & Al-Deyab, S. S. Cellulose nanowhiskers extracted from TEMPO-oxidized jute fibers. *Carbohydr. Polym.* **90**, 1075–1080 (2012).
91. Brito, B. S. L., Pereira, F. V., Putaux, J. L. & Jean, B. Preparation, morphology and structure of cellulose nanocrystals from bamboo fibers. *Cellulose* **19**, 1527–1536 (2012).
92. Yoshiharu, N., Shigenori, K., Masahisa, W. & Takeshi, O. Cellulose microcrystal film of high uniaxial orientation. *Macromolecules* **30**, 6395–6397 (1997).
93. El Achaby, M., Kassab, Z., Aboulkas, A., Gaillard, C. & Barakat, A. Reuse of red algae waste for the production of cellulose nanocrystals and its application in polymer nanocomposites. *Int. J. Biol. Macromol.* **106**, 681–691 (2018).
94. Sugiyama, J., Vuong, R. & Chanzy, H. Electron diffraction study on the two crystalline phases occurring in native cellulose from an algal cell wall. *Macromolecules* **24**, 4168–4175 (1991).
95. Chanzy, H. & Henrissat, B. Electron microscopy study of the enzymic hydrolysis of Valonia cellulose. *Carbohydr. Polym.* **3**, 161–173 (1983).
96. Hirai, A., Inui, O., Horii, F. & Tsuji, M. Phase separation behavior in aqueous suspensions of bacterial cellulose nanocrystals prepared by sulfuric acid treatment. *Langmuir* **25**, 497–502 (2009).
97. Pääkkönen, T. et al. Sustainable high yield route to cellulose nanocrystals from bacterial cellulose. *ACS Sustainable Chem. Eng.* **7**, 14384–14388 (2019).
98. Cranston, E. D. in *TAPPI International Conference on Nanotechnology for Renewable Materials* (2019).
99. Ngo, T., Danumah, C. & Ahvazi, B. in *Nanocellulose and Sustainability* (ed. Lee, K. Y.) 269–287 (CRC, 2018).
100. The University of Maine. The Process Development Center. *UMaine* https://umaine.edu/pdc/nanocellulose/ (2020).
101. Beck, S., Bouchard, J. & Berry, R. Dispersibility in water of dried nanocrystalline cellulose. *Biomacromolecules* **13**, 1486–1494 (2012).
102. Lockhart, J. in *TAPPI International Conference on Nanotechnology for Renewable Materials* (2019).
103. Andrews, M. P. & Morse, T. Method for producing functionalized nanocrystalline cellulose and functionalized nanocrystalline cellulose thereby produced. US Patent 20170260298A1 (2017).
104. McAlpine, S. & Nakoneshny, J. Production of crystalline cellulose. US Patent 20190040158A1 (2019).
105. Standards Council of Canada. Cellulose nanomaterials — test methods for characterization CAN/CSA-Z5100-17 (CSA Group, 2017).
106. Standards Council of Canada. Cellulose nanomaterials — blank detail specification, CAN/CSA-Z5200-17 (CSA Group, 2017).
107. International Organization for Standardization. Nanotechnologies — characterization of cellulose nanocrystals ISO/TR 19716 (ISO, 2016).
108. International Organization for Standardization. Pulp — determination of cellulose nanocrystal sulfur and sulfate half-ester content ISO 21400 (ISO, 2018).
109. International Organization for Standardization. Crystallinity of cellulose nanomaterials by powder X-ray diffraction, ISO/TC 229 – PWI 23361 (in the press).
110. International Organization for Standardization. Nanotechnologies — health and safety practices in occupational settings relevant to nanotechnologies ISO/TR 12885 (ISO, 2018).
111. Standards Council of Canada. Nanotechnologies — exposure control program for engineered nanomaterials in occupational settings CAN/CSA Z12885-12 (CSA Group, 2017).
112. Lin, N. & Dufresne, A. Surface chemistry, morphological analysis and properties of cellulose nanocrystals with gradiented sulfation degrees. *Nanoscale* **6**, 5384–5393 (2014).
113. Heggset, E. B., Chinga-Carrasco, G. & Syverud, K. Temperature stability of nanocellulose dispersions. *Carbohydr. Polym.* **157**, 114–121 (2017).
114. Molnes, S. N., Paso, K. G., Strand, S. & Syverud, K. The effects of pH, time and temperature on the stability and viscosity of cellulose nanocrystal (CNC) dispersions: implications for use in enhanced oil recovery. *Cellulose* **24**, 4479–4491 (2017).
115. Zhong, L., Fu, S., Peng, X., Zhan, H. & Sun, R. Colloidal stability of negatively charged cellulose nanocrystalline in aqueous systems. *Carbohydr. Polym.* **90**, 644–649 (2012).
116. Shafiei-Sabet, S., Hamad, W. Y. & Hatzikiriakos, S. G. Ionic strength effects on the microstructure and shear rheology of cellulose nanocrystal suspensions. *Cellulose* **21**, 3347–3359 (2014).
117. De Figueirêdo, M. C. B. et al. Life cycle assessment of cellulose nanowhiskers. *J. Clean. Prod.* **35**, 130–139 (2012).
118. Leão, R. M., Milêo, P. C., Maia, J. M. L. L. & Luz, S. M. Environmental and technical feasibility of cellulose nanocrystal manufacturing from sugarcane bagasse. *Carbohydr. Polym.* **175**, 518–529 (2017).
119. Bajpai, P. *Green Chemistry and Sustainability in Pulp and Paper Industry* (Springer, 2015).
120. Li, Q., McGinnis, S., Sydnor, C., Wong, A. & Renneckar, S. Nanocellulose life cycle assessment. *ACS Sustain. Chem. Eng.* **1**, 919–928 (2013).
121. Wang, R., Chen, L., Zhu, J. Y. & Yang, R. Tailored and integrated production of carboxylated cellulose nanocrystals (CNC) with nanofibrils (CNF) through maleic acid hydrolysis. *ChemNanoMat* **3**, 328–335 (2017).
122. Bian, H., Chen, L., Dai, H. & Zhu, J. Y. Integrated production of lignin containing cellulose nanocrystals (LCNC) and nanofibrils (LCNF) using an easily recyclable di-carboxylic acid. *Carbohydr. Polym.* **167**, 167–176 (2017).
123. Park, N.-M., Choi, S., Oh, J. E. & Youn Hwang, D. Facile extraction of cellulose nanocrystals. *Carbohydr. Polym.* **223**, 115114 (2019).
124. Pääkkönen, T. et al. From vapour to gas: optimising cellulose degradation with gaseous HCl. *React. Chem. Eng.* **3**, 312–318 (2018).
125. Guo, J., Guo, X., Wang, S. & Yin, Y. Effects of ultrasonic treatment during acid hydrolysis on the yield, particle size and structure of cellulose nanocrystals. *Carbohydr. Polym.* **135**, 248–255 (2016).
126. Jakubek, Z. J. et al. Characterization challenges for a cellulose nanocrystal reference material: dispersion and particle size distributions. *J. Nanopart. Res.* **20**, 98 (2018).
127. Brinkmann, A. et al. Correlating cellulose nanocrystal particle size and surface area. *Langmuir* **32**, 6105–6114 (2016).
128. Elazzouzi-Hafraoui, S. et al. The shape and size distribution of crystalline nanoparticles prepared by acid hydrolysis of native cellulose. *Biomacromolecules* **9**, 57–65 (2008).
129. Garcia de Rodriguez, N. L., Thielemans, W. & Dufresne, A. Sisal cellulose whiskers reinforced polyvinyl acetate nanocomposites. *Cellulose* **13**, 261–270 (2006).
130. Beck-Candanedo, S., Roman, M. & Gray, D. Effect of conditions on the properties behavior of wood cellulose nanocrystals suspensions. *Biomacromolecules* **6**, 1048–1054 (2005).
131. Wu, Q. et al. Rheological behavior of cellulose nanocrystal suspension: Influence of concentration and aspect ratio. *J. Appl. Polym. Sci.* **131**, 40525 (2014).
132. Frka-Petesic, B., Jean, B. & Heux, L. First experimental evidence of a giant permanent electric-dipole moment in cellulose nanocrystals. *EPL* **107**, 28006 (2014).
133. Sugiyama, J., Chanzy, H. & Maret, G. Orientation of cellulose microcrystals by strong magnetic fields. *Macromolecules* **25**, 4232–4234 (1992).
134. Revol, J.-F. et al. Chiral nematic suspensions of cellulose crystallites; phase separation and magnetic field orientation. *Liq. Cryst.* **16**, 127–134 (1994).
135. Frka-Petesic, B., Sugiyama, J., Kimura, S., Chanzy, H. & Maret, G. Negative diamagnetic anisotropy and birefringence of cellulose nanocrystals. *Macromolecules* **48**, 8844–8857 (2015).
136. De France, K. J., Yager, K. G., Hoare, T. & Cranston, E. D. Cooperative ordering and kinetics of cellulose nanocrystal alignment in a magnetic field. *Langmuir* **32**, 7564–7571 (2016).
137. Frka-Petesic, B., Guidetti, G., Kamita, G. & Vignolini, S. Controlling the photonic properties of cholesteric cellulose nanocrystal films with magnets. *Adv. Mater.* **29**, 1701469 (2017).
138. Flauzino Neto, W. P. et al. Mechanical properties of natural rubber nanocomposites reinforced with high aspect ratio cellulose nanocrystals isolated from soy hulls. *Carbohydr. Polym.* **153**, 143–152 (2016).
139. Mariano, M., Chirat, C., El Kissi, N. & Dufresne, A. Impact of cellulose nanocrystal aspect ratio on crystallization and reinforcement of poly(butylene adipate-co-terephthalate). *J. Polym. Sci. Part B Polym. Phys.* **54**, 2284–2297 (2016).
140. Rusli, R., Shanmuganathan, K., Rowan, S. J., Weder, C. & Eichhorn, S. J. Stress transfer in cellulose nanowhisker composites - Influence of whisker aspect ratio and surface charge. *Biomacromolecules* **12**, 1363–1369 (2011).
141. Kalashnikova, I., Bizot, H., Bertoncini, P., Cathala, B. & Capron, I. Cellulosic nanorods of various aspect ratios for oil in water Pickering emulsions. *Soft Matter* **9**, 952–959 (2013).
142. Kalashnikova, I., Bizot, H., Cathala, B. & Capron, I. Modulation of cellulose nanocrystals amphiphilic properties to stabilize oil/water interface. *Biomacromolecules* **13**, 267–275 (2012).
143. Grønli, M., Antal, M. J. & Várhegyi, G. A round-robin study of cellulose pyrolysis kinetics by thermogravimetry. *Ind. Eng. Chem. Res.* **38**, 2238–2244 (1999).
144. Roman, M. & Winter, W. T. Effect of sulfate groups from sulfuric acid hydrolysis on the thermal degradation behavior of bacterial cellulose. *Biomacromolecules* **5**, 1671–1677 (2004).
145. Scheirs, J., Camino, G. & Tumiatti, W. Overview of water evolution during the thermal degradation of cellulose. *Eur. Polym. J.* **37**, 933–942 (2001).
146. Beck, S. & Bouchard, J. Auto-catalyzed acidic desulfation of cellulose nanocrystals. *Nord. Pulp Pap. Res. J.* **29**, 6–14 (2014).
147. Kaur, B., Gur, I. S. & Bhatnagar, H. L. Thermal degradation studies of cellulose phosphates and cellulose thiophosphates. *Angew. Makromol. Chem.* **147**, 157–183 (1987).
148. Fiss, B. G., Hatherly, L., Stein, R. S., Friščić, T. & Moores, A. Mechanochemical phosphorylation of polymers and synthesis of flame-retardant cellulose nanocrystals. *ACS Sustain. Chem. Eng.* **7**, 7951–7959 (2019).
149. Matsuoka, S., Kawamoto, H. & Saka, S. What is active cellulose in pyrolysis? An approach based on reactivity of cellulose reducing end. *J. Anal. Appl. Pyrolysis* **106**, 138–146 (2014).
150. Heise, K. et al. Chemical modification of cellulose nanocrystal reducing end-groups. *Angew. Chem. Int. Ed.* https://doi.org/10.1002/ange.202002433 (2020).

151. Spinella, S. et al. Concurrent cellulose hydrolysis and esterification to prepare a surface-modified cellulose nanocrystal decorated with carboxylic acid moieties. *ACS Sustain. Chem. Eng.* **4**, 1538–1550 (2016).
152. Niinivaara, E., Faustini, M., Tammelin, T. & Kontturi, E. Water vapor uptake of ultrathin films of biologically derived nanocrystals: quantitative assessment with quartz crystal microbalance and spectroscopic ellipsometry. *Langmuir* **31**, 12170–12176 (2015).
153. Lindman, B., Karlström, G. & Stigsson, L. On the mechanism of dissolution of cellulose. *J. Mol. Liq.* **156**, 76–81 (2010).
154. Medronho, B., Romano, A., Miguel, M. G., Stigsson, L. & Lindman, B. Rationalizing cellulose (in)solubility: reviewing basic physicochemical aspects and role of hydrophobic interactions. *Cellulose* **19**, 581–587 (2012).
155. Lindh, E. L., Terenzi, C., Salmén, L. & Furó, I. Water in cellulose: evidence and identification of immobile and mobile adsorbed phases by ^{2}H MAS NMR. *Phys. Chem. Chem. Phys.* **19**, 4360–4369 (2017).
156. Lemke, C. H., Dong, R. Y., Michal, C. A. & Hamad, W. Y. New insights into nano-crystalline cellulose structure and morphology based on solid-state NMR. *Cellulose* **19**, 1619–1629 (2012).
157. Dong, X. M. & Gray, D. G. Effect of counterions on ordered phase formation in suspensions of charged rodlike cellulose crystallites. *Langmuir* **13**, 2404–2409 (1997).
158. Chen, Y. et al. Solution-phase EPR studies of single-walled carbon nanotubes. *Chem. Phys. Lett.* **299**, 532–535 (1999).
159. Reid, M. S., Villalobos, M. & Cranston, E. D. Cellulose nanocrystal interactions probed by thin film swelling to predict dispersibility. *Nanoscale* **8**, 12247–12257 (2016).
160. van der Berg, O., Capadona, J. R. & Weder, C. Preparation of homogeneous dispersions of tunicate cellulose whiskers in organic solvents. *Biomacromolecules* **8**, 1353–1357 (2007).
161. Mazeau, K. On the external morphology of native cellulose microfibrils. *Carbohydr. Polym.* **84**, 524–532 (2011).
162. Kedzior, S. A. et al. Incorporating cellulose nanocrystals into the core of polymer latex particles via polymer grafting. *ACS Macro Lett.* **7**, 990–996 (2018).
163. Hatton, F. L., Kedzior, S. A., Cranston, E. D. & Carlmark, A. Grafting-from cellulose nanocrystals via photoinduced Cu-mediated reversible-deactivation radical polymerization. *Carbohydr. Polym.* **157**, 1033–1040 (2017).
164. Braun, B. & Dorgan, J. R. Single-step method for the isolation and surface functionalization of cellulosic nanowhiskers. *Biomacromolecules* **10**, 334–341 (2009).
165. Ojala, J., Sirviö, J. A. & Liimatainen, H. Preparation of cellulose nanocrystals from lignin-rich reject material for oil emulsification in an aqueous environment. *Cellulose* **25**, 293–304 (2018).
166. Wei, L., Agarwal, U. P., Matuana, L., Sabo, R. C. & Stark, N. M. Performance of high lignin content cellulose nanocrystals in poly(lactic acid). *Polymer* **135**, 305–313 (2018).
167. Yang, X. & Cranston, E. D. Chemically cross-linked cellulose nanocrystal aerogels with shape recovery and superabsorbent properties. *Chem. Mater.* **26**, 6016–6025 (2014).
168. Osorio, D. A., Seifried, B., Moquin, P., Grandfield, K. & Cranston, E. D. Morphology of cross-linked cellulose nanocrystal aerogels: cryo-templating versus pressurized gas expansion processing. *J. Mater. Sci.* **53**, 9842–9860 (2018).
169. Sun, B., Hou, Q., Liu, Z. & Ni, Y. Sodium periodate oxidation of cellulose nanocrystal and its application as a paper wet strength additive. *Cellulose* **22**, 1135–1146 (2015).
170. Eyley, S. S. & Thielemans, W. Surface modification of cellulose nanocrystals. *Nanoscale* **6**, 7764–7779 (2014).
171. Zoppe, J. O. et al. Effect of surface charge on surface-initiated atom transfer radical polymerization from cellulose nanocrystals in aqueous media. *Biomacromolecules* **17**, 1404–1413 (2016).
172. Drogat, N. et al. Antimicrobial silver nanoparticles generated on cellulose nanocrystals. *J. Nanopart. Res.* **13**, 1557–1562 (2011).
173. Kaushik, M. & Moores, A. Review: nanocelluloses as versatile supports for metal nanoparticles and their applications in catalysis. *Green Chem.* **18**, 622–637 (2016).
174. Tang, J., Sisler, J., Grishkewich, N. & Tam, K. C. Functionalization of cellulose nanocrystals for advanced applications. *J. Colloid Interface Sci.* **494**, 397–409 (2017).
175. Richardson, J. J. et al. Continuous metal-organic framework biomineralization on cellulose nanocrystals: extrusion of functional composite filaments. *ACS Sustain. Chem. Eng.* **7**, 6287–6294 (2019).
176. Azzam, F., Heux, L., Jean, B. & Putaux, J.-L. Preparation by grafting onto, characterization and properties of thermally responsive polymer-decorated cellulose nanocrystals. *Biomacromolecules* **11**, 3652–3659 (2010).
177. Kloser, E. & Gray, D. G. Surface grafting of cellulose nanocrystals with poly(ethylene oxide) in aqueous media. *Langmuir* **26**, 13450–13456 (2010).
178. Yang, H., Chen, D. & van de Ven, T. G. M. Preparation and characterization of sterically stabilized nanocrystalline cellulose obtained by periodate oxidation of cellulose fibers. *Cellulose* **22**, 1743–1752 (2015).
179. Yang, H., Tejado, A., Alam, N., Antal, M. & Van De Ven, T. G. M. Films prepared from electrosterically stabilized nanocrystalline cellulose. *Langmuir* **28**, 7834–7842 (2012).
180. Yang, H., Alam, M. N. & van de Ven, T. G. M. Highly charged nanocrystalline cellulose and dicarboxylated cellulose from periodate and chlorite oxidized cellulose fibers. *Cellulose* **20**, 1865–1875 (2013).
181. Campano, C., Lopez-Exposito, P., Blanco, A., Negro, C. & van de Ven, T. G. M. Hairy cationic nanocrystalline cellulose as a novel flocculant of clay. *J. Colloid Interface Sci.* **545**, 153–161 (2019).
182. Lopez-Exposito, P., Campano, C., van de Ven, T. G. M., Negro, C. & Blanco, A. Microalgae harvesting with the novel flocculant hairy cationic nanocrystalline cellulose. *Colloids Surf. B* **178**, 329–336 (2019).
183. Jorfi, M. & Foster, E. J. Recent advances in nanocellulose for biomedical applications. *J. Appl. Polym. Sci.* **132**, 41719 (2015).
184. Osorio, D. A. et al. Cross-linked cellulose nanocrystal aerogels as viable bone tissue scaffolds. *Acta Biomater.* **87**, 152–165 (2019).
185. De France, K. J. et al. Tissue response and biodistribution of injectable cellulose nanocrystal composite hydrogels. *ACS Biomater. Sci. Eng.* **5**, 2235–2246 (2019).
186. Yanamala, N. et al. In vivo evaluation of the pulmonary toxicity of cellulose nanocrystals: A renewable and sustainable nanomaterial of the future. *ACS Sustain. Chem. Eng.* **2**, 1691–1698 (2014).
187. Pelegrini, B. L. et al. Cellulose nanocrystals as a sustainable raw material: Cytotoxicity and applications on healthcare technology. *Macromol. Mater. Eng.* **304**, 1900092 (2019).
188. Kovacs, T. et al. An ecotoxicological characterization of nanocrystalline cellulose (NCC). *Nanotoxicology* **4**, 255–270 (2010).
189. Hanif, Z., Ahmed, F. R., Shin, S. W., Kim, Y. K. & Um, S. H. Size- and dose-dependent toxicity of cellulose nanocrystals (CNC) on human fibroblasts and colon adenocarcinoma. *Colloids Surf. B* **119**, 162–165 (2014).
190. Hosseinidoust, Z., Alam, M. N., Sim, G., Tufenkji, N. & Van De Ven, T. G. M. Cellulose nanocrystals with tunable surface charge for nanomedicine. *Nanoscale* **7**, 16647–16657 (2015).
191. Habibi, Y., Lucia, L. A. & Rojas, O. J. Cellulose nanocrystals: chemistry, self-assembly, and applications. *Chem. Rev.* **110**, 3479–3500 (2010).
192. Lagerwall, J. P. F. et al. Cellulose nanocrystal-based materials: From liquid crystal self-assembly and glass formation to multifunctional thin films. *NPG Asia Mater.* **6**, e80 (2014).
193. Revol, J.-F., Godbout, D. L. & Gray, D. G. Solidified liquid crystals of cellulose with optically variable properties. US Patent 5629055A (1994).
194. Beck, S., Bouchard, J. & Berry, R. Iridescent solid nanocrystalline cellulose films incorporating patterns and method for their production. US Patent 20100151159A1 (2009).
195. Araki, J., Wada, M., Kuga, S. & Okano, T. Flow properties of microcrystalline cellulose suspension prepared by acid treatment of native cellulose. *Colloids Surf. A* **142**, 75–82 (1998).
196. Liu, Y. et al. A novel approach for the preparation of nanocrystalline cellulose by using phosphotungstic acid. *Carbohydr. Polym.* **110**, 415–422 (2014).
197. Vasconcelos, N. F. et al. Bacterial cellulose nanocrystals produced under different hydrolysis conditions: Properties and morphological features. *Carbohydr. Polym.* **155**, 425–431 (2017).
198. Cheng, M., Qin, Z., Chen, Y., Liu, J. & Ren, Z. Facile one-step extraction and oxidative carboxylation of cellulose nanocrystals through hydrothermal reaction by using mixed inorganic acids. *Cellulose* **24**, 3243–3254 (2017).
199. Lalia, B. S., Samad, Y. A. & Hashaikeh, R. Nanocrystalline-cellulose-reinforced poly(vinylidenefluoride-co-hexafluoropropylene) nanocomposite films as a separator for lithium ion batteries. *J. Appl. Polym. Sci.* **126**, E442–E448 (2012).
200. Li, R. et al. Cellulose whiskers extracted from mulberry: a novel biomass production. *Carbohydr. Polym.* **76**, 94–99 (2009).
201. Shaheen, T. I. & Emam, H. E. Sono-chemical synthesis of cellulose nanocrystals from wood sawdust using acid hydrolysis. *Int. J. Biol. Macromol.* **107**, 1599–1606 (2018).
202. Le Normand, M., Moriana, R. & Ek, M. Isolation and characterization of cellulose nanocrystals from spruce bark in a biorefinery perspective. *Carbohydr. Polym.* **111**, 979–987 (2014).
203. Morais, J. P. S. et al. Extraction and characterization of nanocellulose structures from raw cotton linter. *Carbohydr. Polym.* **91**, 229–235 (2013).
204. Wang, Z., Yao, Z. J., Zhou, J. & Zhang, Y. Reuse of waste cotton cloth for the extraction of cellulose nanocrystals. *Carbohydr. Polym.* **157**, 945–952 (2017).
205. Edgar, C. D. & Gray, D. G. Smooth model cellulose I surfaces from nanocrystal suspensions. *Cellulose* **10**, 299–306 (2003).
206. Nascimento, S. A. & Rezende, C. A. Combined approaches to obtain cellulose nanocrystals, nanofibrils and fermentable sugars from elephant grass. *Carbohydr. Polym.* **180**, 38–45 (2018).
207. Cao, X., Dong, H. & Li, C. M. New nanocomposite materials reinforced with flax cellulose nanocrystals in waterborne polyurethane. *Biomacromolecules* **8**, 899–904 (2007).
208. Cao, X., Chen, Y., Chang, P. R., Stumborg, M. & Huneault, M. A. Green composites reinforced with hemp nanocrystals in plasticized starch. *J. Appl. Polym. Sci.* **109**, 3804–3810 (2008).
209. Luzi, F. et al. Optimized extraction of cellulose nanocrystals from pristine and carded hemp fibres. *Ind. Crop. Prod.* **56**, 175–186 (2014).
210. Sheltami, R. M., Abdullah, I., Ahmad, I., Dufresne, A. & Kargarzadeh, H. Extraction of cellulose nanocrystals from mengkuang leaves (Pandanus tectorius). *Carbohydr. Polym.* **88**, 772–779 (2012).
211. Habibi, Y. et al. Bionanocomposites based on poly(ε-caprolactone)-grafted cellulose nanocrystals by ring-opening polymerization. *J. Mater. Chem.* **18**, 5002–5010 (2008).
212. César, N. R., Pereira-da-Silva, M. A., Botaro, V. R. & de Menezes, A. J. Cellulose nanocrystals from natural fiber of the macrophyte Typha domingensis: extraction and characterization. *Cellulose* **22**, 449–460 (2015).
213. Fortunati, E. et al. Revalorization of sunflower stalks as novel sources of cellulose nanofibrils and nanocrystals and their effect on wheat gluten bionanocomposite properties. *Carbohydr. Polym.* **149**, 357–368 (2016).
214. Mueller, S., Weder, C. & Foster, E. J. Isolation of cellulose nanocrystals from pseudostems of banana plants. *RSC Adv.* **4**, 907–915 (2014).
215. Rosa, M. F. et al. Cellulose nanowhiskers from coconut husk fibers: effect of preparation conditions on their thermal and morphological behavior. *Carbohydr. Polym.* **81**, 83–92 (2010).
216. Collazo-Bigliardi, S., Ortega-Toro, R. & Chiralt Boix, A. Isolation and characterisation of microcrystalline cellulose and cellulose nanocrystals from coffee husk and comparative study with rice husk. *Carbohydr. Polym.* **191**, 205–215 (2018).
217. Silvério, H. A., Flauzino Neto, W. P., Dantas, N. O. & Pasquini, D. Extraction and characterization of cellulose nanocrystals from corncob for application as reinforcing agent in nanocomposites. *Ind. Crop. Prod.* **44**, 427–436 (2013).
218. Kallel, F. et al. Isolation and structural characterization of cellulose nanocrystals extracted from garlic straw residues. *Ind. Crop. Prod.* **87**, 287–296 (2016).
219. Henrique, M. A., Silvério, H. A., Flauzino Neto, W. P. & Pasquini, D. Valorization of an agro-industrial waste, mango seed, by the extraction and characterization of its cellulose nanocrystals. *J. Environ. Manage.* **121**, 202–209 (2013).
220. Rhim, J. W., Reddy, J. P. & Luo, X. Isolation of cellulose nanocrystals from onion skin and their utilization for the preparation of agar-based bio-nanocomposites films. *Cellulose* **22**, 407–420 (2015).

221. Wijaya, C. J. et al. Cellulose nanocrystals from passion fruit peels waste as antibiotic drug carrier. *Carbohydr. Polym.* **175**, 370–376 (2017).
222. Chen, Y., Liu, C., Chang, P. R., Cao, X. & Anderson, D. P. Bionanocomposites based on pea starch and cellulose nanowhiskers hydrolyzed from pea hull fibre: effect of hydrolysis time. *Carbohydr. Polym.* **76**, 607–615 (2009).
223. Dai, H., Ou, S., Huang, Y. & Huang, H. Utilization of pineapple peel for production of nanocellulose and film application. *Cellulose* **25**, 1743–1756 (2018).
224. Marett, J., Aning, A. & Foster, E. J. The isolation of cellulose nanocrystals from pistachio shells via acid hydrolysis. *Ind. Crop. Prod.* **109**, 869–874 (2017).
225. Chen, D., Lawton, D., Thompson, M. R. & Liu, Q. Biocomposites reinforced with cellulose nanocrystals derived from potato peel waste. *Carbohydr. Polym.* **90**, 709–716 (2012).
226. Lu, P. & Hsieh, Y. L. O. Preparation and characterization of cellulose nanocrystals from rice straw. *Carbohydr. Polym.* **87**, 564–573 (2012).
227. Flauzino Neto, W. P., Silvério, H. A., Dantas, N. O. & Pasquini, D. Extraction and characterization of cellulose nanocrystals from agro-industrial residue - soy hulls. *Ind. Crop. Prod.* **42**, 480–488 (2013).
228. Favier, V., Chanzy, H. & Cavaillé, J. Y. Polymer nanocomposites reinforced by cellulose whiskers. *Macromolecules* **28**, 6365–6367 (1995).
229. Retsina, T. & Pylkkanen, V. Method for the production of fermentable sugars and cellulose from lignocellulosic material. US Patent 8030039B1 (2011).
230. Retsina, T., Pylkkanen, V. & van Heiningen, A. Method for vapor phase pulping with alcohol, sulfur dioxide and ammonia. US Patent 8038842B2 (2011).
231. Retsina, T., Pylkkanen, V. & van Heiningen, A. Method for vapor phase pulping with alcohol and sulfur dioxide. US Patent 20120305207A1 (2012).
232. Retsina, T. & Pylkkanen, V. Separation of lignin from hydrolyzate.US Patent 8864941B2 (2013).
233. Choi, Y. & Simonsen, J. Cellulose nanocrystal-filled carboxymethyl cellulose nanocomposites. *J. Nanosci. Nanotechnol.* **6**, 633–639 (2006).
234. Heath, L. & Thielemans, W. Cellulose nanowhisker aerogels. *Green. Chem.* **12**, 1448–1453 (2010).
235. Liew, S. Y., Thielemans, W. & Walsh, D. A. Electrochemical capacitance of nanocomposite polypyrrole/cellulose films. *J. Phys. Chem. C.* **114**, 17926–17933 (2010).
236. Jackson, J. K. et al. The use of nanocrystalline cellulose for the binding and controlled release of drugs. *Int. J. Nanomed.* **6**, 321–330 (2011).
237. Kalashnikova, I., Bizot, H., Cathala, B. & Capron, I. New Pickering emulsions stabilized by bacterial cellulose nanocrystals. *Langmuir* **27**, 7471–7479 (2011).
238. Cao, Y., Weiss, W. J., Youngblood, J., Moon, R. & Zavattieri, P. in *Production and Applications of Cellulose Nanomaterial* (eds Postek, M. T., Moon, R. J., Rudie, A. W. & Bilodeau, M. A.) 135–136 (TAPPI, 2013).

Acknowledgements
The authors thank E. Niinivaara and G. Delepierre for drawing chemical structures. E.D.C. is grateful for financial support and recognition through the Early Researcher awards from the Ontario Ministry of Research and Innovation, the Canada Research Chairs programme and the University of British Columbia's President's Excellence Chair initiative. McMaster University (Faculty of Engineering), the University of British Columbia (Faculty of Applied Science and Faculty of Forestry) and the BioProducts Institute (http://bpi.ubc.ca) are gratefully acknowledged for support. This work was funded through Natural Sciences and Engineering Research Council of Canada (NSERC) Discovery Grant RGPIN-2017-05252 to E.D.C. and an NSERC Alexander Graham Bell Canada Graduate Scholarship to O.M.V.

Author contributions
O.M.V. and E.D.C developed the outline and wrote the manuscript in collaboration. O.M.V. compiled all data in tables. O.M.V. and E.D.C revised the manuscript on the basis of reviewer and editorial suggestions.

Competing interests
The authors declare no competing interests.

Publisher's note
Springer Nature remains neutral with regard to jurisdictional claims in published maps and institutional affiliations.